CONSTRUCTION MATERIALS CONSULTANTS, INC.

Investigation of Concrete Surface Cracking by Laboratory Examinations of Three Concrete Cores

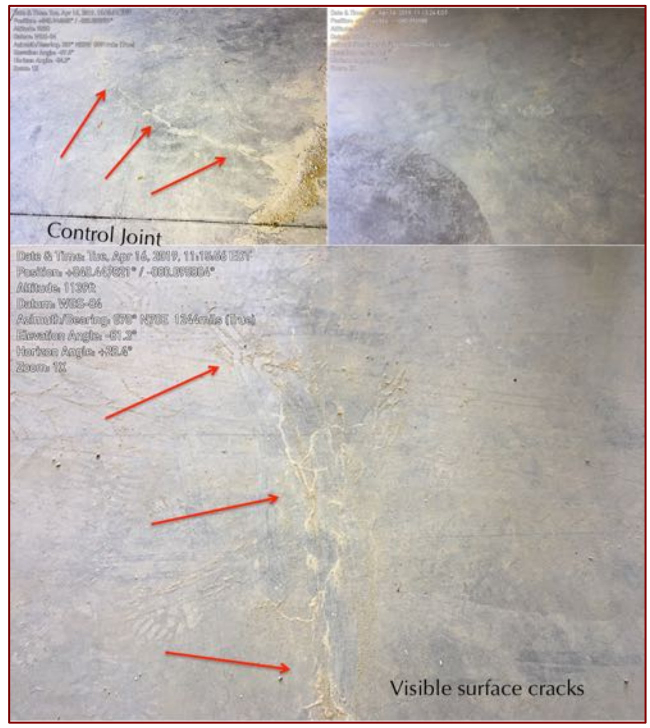

Appliance II
251 Bilmar Drive
Pittsburgh, PA 15205

April 22, 2019
CMC 0419115

TABLE OF CONTENTS

EXECUTIVE SUMMARY

The purpose of this present study is to investigate surface cracking of an indoor concrete slab that was placed in November of 2018 and developed surface cracking by December 2018 and January 2019. The slab, though indoor, was reportedly placed without any protection from freezing during winter weather placement. The slab was placed on a vapor retarder and received a "burned" hard steel trowel finish. A 3500-psi, non-air-entrained, fiberglass-reinforced concrete mix with added 2% non-chloride accelerator, and superplastisizer was used that provided a slump of 6 to 7.5 inches and fresh air content ranges of 1.2 to 1.8 percent. Cylinder breaks showed in excess of 3500 psi strength by 7 days (as opposed to that 'design strength' in 28 days) and a 170 percent increase in compressive strength to around 6000 psi in 28 days to increase the elastic modulus of concrete significantly higher than a modulus more consistent with the reported design mix. Project specification reportedly called for saw-cut control joints placed at 15 ft. intervals, which appeared to be more like 12 to 13 ft. spacing and 1.5 to 2 in. deep. Two cores, Nos. 1 and 3 were collected from areas that exhibit cracking, and one core No. 2 was from a control area that seemed to be in better condition.

The cores were tested by detailed petrographic examinations *a la* ASTM C 856 and chemical profiles of water-soluble chloride, sulfate and alkalis through depths of the cores by potentiometric titration (for chloride) and ion chromatography (for anions and cations) to determine any moisture migration issues to cause differential moisture conditions between top and bottom ends of slab. Based on petrographic examinations, concretes in all three cores are found to be compositionally similar and made using: (a) crushed limestone-dolomite coarse aggregates having nominal maximum sizes of 1 in. (25 mm), (b) natural siliceous-calcareous sand fine aggregates having nominal maximum sizes of $^{3}/_{8}$ in. (9.5 mm), (c) cementitious materials contents similar in all three cores and estimated to be equivalent to 7 to $7^{1}/_{2}$ bags of Portland cement per cubic yard of which 25 to 30 percent is estimated to be ground granulated blast furnace slag, (d) water-cementitious materials ratios estimated to be less than 0.40 at the top 5 mm of the finished surface regions due to hard trowel-finishing operations (that have washed some mix water out of the surface) and 0.40 to 0.44 in the interior bodies of the cores, (e) air contents similar in all three cores and estimated to be 1 to 2 percent, and (e) fine, hair-like polypropylene-type synthetic fibers uniformly distributed throughout the concretes. Overall concretes in all three cores are dense and well-consolidated. Both coarse and fine aggregates are well-graded, well-distributed, and have been present in sound conditions without any contributions to the reported and observed cracking of the concrete slab. There is no evidence of any unsoundness of aggregates or any chemical deterioration of concrete found in the cores to explain the observed cracking of slab.

Core 1 showed a major visible crack at one edge that extended to a depth of 2 inches. Core 3 showed almost full-depth cracking, appeared as fine hairline cracks as well as network of craze cracking on the top surface. By contrast, top surface and side of Core 2 showed no visible cracking; however, the top near-surface region of Core 2 showed a small surface-parallel microcrack at a depth of 10 to 15 mm. Therefore, despite difference in appearance of visible cracking in the field, concrete in all three cores appeared to have undergone some micro to macrocracking at variable degrees – from low at the location of Core 2 to severe at the location of Core 3.

Evidences helpful to investigate reasons for surface cracking of slab include: (i) configuration of the cracks, e.g., surface patters and pathways through the cores, e.g., if mostly around the aggregates but some transecting the aggregates indicating its development after the major aggregate-paste bond was developed (i.e. after a strength of at least 2500 psi); (ii) concrete mix, (iii) slab thickness; (iii) depth, spacing, and timing of placement of control joints since placement; (iv) compressive strength and modulus of elasticity of concrete and their influence on the curling potential of slab; (v) location of wire mesh and reinforcement in the slab, e.g., location of mesh at the bottom surface end of slab instead of at the top half or preferably at the top one third the thickness of the slab increases shrinkage-related cracking at the surface; (vi) possible lack of adequate reinforcement; (vii) differential drying of slab between the top and bottom ends, e.g., placement of slab on a vapor retarder reduces loss of moisture through the base and ambient relative humidity above the slab controls the rate of evaporation of moisture from the surface; (viii) possible early freezing of slab after placement in winter weather conditions in November of 2018 where the slab was not protected from freezing with an external heating, especially due to the observed non-air-entrained nature of the concrete which increases vulnerability to cracking due to freezing at critically saturated conditions.

Two types of cracks are observed in three cores: (a) the first type is oriented perpendicular to the trowel-finished surface, appeared as visible cracks on the finished surface from fine craze cracks to wider visible cracks, extended to variable depths from 2 inches in Core 1 to almost the entire depth in Core 3, whereas (b) the second type is situated near the finished surface, within the top 1 in. of the finished surface from a depth of 10 to 15 mm in Core 2 to 25 to 30 mm in Core 3. Based on detailed petrographic examinations the former type of vertical cracking through slab thickness is judged to be due to unaccommodative drying shrinkage of concrete, whereas the latter type of near-surface near—horizontal cracks are due to a combination of drying shrinkage and early freezing of a non-air-entrained concrete immediately after placement in November without any reported heating to prevent freezing of concrete at the plastic or semi plastic state.

Investigations of ALL these evidence lead to the conclusion that the observed cracking is NOT due to the concrete materials itself but due to either one or a combination of the following:

a. Unaccommodative drying shrinkage of the slab especially due to the higher-than-necessary strength and modulus of elasticity of slab than that consistent with a 3500-psi mix, along with other potential reasons, e.g., lack of adequate reinforcement or placement of reinforcement and mesh at the bottom halves of slab than the top, delayed placement of control joints, inadequate depths of joints, etc. many of which are not possible to investigate in the present laboratory study except from background information provided,
b. Possible curling due to differential drying shrinkage of slab between the top and bottom surfaces, and
c. Possible freezing of the slab at an early age to develop some near-surface surface-parallel microcracking as seen within the top 1 in. in Cores 2 and 3 of the slab surface – all of these mechanisms in combination, or in isolation can develop the observed cracking in the slab.

Based on: (i) review of field photographs and background information provided with the sample; (ii) examination of field photographs of concrete surface cracking, (iii) examination of the configuration of the major visible vertical through-depth crack in Cores 1 and 3, (iv) petrographic examination of sound condition of the concrete away from the cracks with no evidence of any chemical deteriorations to cause the cracks in the first place, (v) along with sound condition of concrete ingredients and normal mix proportions (cement content, water-cement ratio, etc.), where neither the concrete materials nor the proportions have contributed to the cracking, *the observed and reported cracking in the concrete slab was judged to be due to accommodative drying shrinkage of concrete, which may or may not have been aggravated by some additional curling of the slab due to differential drying shrinkage between the top and bottom surfaces of the slab, along with possible early freezing of a non-air-entrained concrete after placement in a winter weather condition without any reported heated enclosures.*

Reasons that could contribute to drying shrinkage and/or curling-related cracking, and, early freezing-related cracking of the slab include:

a. Differential shrinkage of the concrete at the top and bottom ends and possible curling of the slab, especially if the slab was exposed to temperature and/or moisture differential between the top and bottom surfaces, i.e. if the slab was exposed to open air for moisture evaporation (especially in a hot, windy, or dry environment), and was not protected or prevented from moisture loss at the top finished surface region, especially when the slab was placed on a vapor retarder to prevent any moisture loss at the bottom end except only through the top thus to create a moisture gradient, where there is no possibility of drying of the slab from the bottom end as fast as from the top; hence, differential drying was quite possible under this situation, which could have led to the observed cracking of the slab – adequate curing was needed after placement to prevent drying from the top.

b. Inadequate presence, wide spacing, shallow depths, or late placement of control joints in the slab, which were either inactive or did not effectively control shrinkage-related cracking at the joint locations rather than elsewhere in the slab, which has caused development of visible major shrinkage cracks in the slab. For an observed 5 to 6 in. thickness of the slab (from the thicknesses of the cores), the reported 12 to 13 ft. spacing of control joints and 1.5 to 2 in. depths of joints are acceptable. However, deviations from the reported spacing and/or depths of joints (wider spaced joints and/or shallow-depth joints) could contribute to some uncontrolled shrinkage cracking.

c. Inadequate amount of wire mesh and steel reinforcement in the slab, especially due to the absence of any mesh or reinforcing steel in the cores examined. Presence of polypropylene-type fiber reinforcement in the concrete however should provide some resistance to shrinkage-related cracking.

d. The reported compressive strength test results of cylinders are around 6000 psi at 28 days, i.e. noticeably higher than the reported 28-day design strength of 3500 psi. Such higher than needed strength would increase the modulus of elasticity of concrete, which would increase the potential for curling and curling-related cracking of slab.

e. The reported mix design of the concrete called for a non-air-entrained concrete, which if placed in areas not well protected from freezing during November 2018 placement could have developed some freezing-relate cracking, especially the near-surface cracks found within the top 1 in. in Cores 2 and 3.

f. Any other non-concrete-related reasons, which are not possible to investigate from the present study.

From the present study, the concrete materials *per se* are judged to be sound and did not contribute to the cracking.

INTRODUCTION

Reported herein are the results of detailed laboratory examinations of three (3) hardened concrete cores identified as Nos. 1, 2, and 3 received from an indoor concrete slab at Appliance II located in Pittsburgh, Pennsylvania.

BACKGROUND INFORMATION

The cores were, reportedly, obtained from indoor slab-on-grade that has experienced cracking. Figures 1 through 4 provide field inspection reports, drawing of core locations, field test reports, etc. that were supplied with the cores.

The subject slab was reportedly placed on November 10 and 11 of 2018 and cracking was first noticed in December 2018 and January 2019, i.e. 1 to 2 months after placement. Additionally, it was reported that there were no walls up for protection from wind/wind chill etc., no tenting or applied heat, only tarps for covering while the slab was placed. The slab was reportedly of a 3500-psi, non-air-entrained, fiberglass-reinforced concrete mix with added 2% non-chloride accelerator, and superplastisizer that has received a "burned" and steel hard trowel finish. Project specification reportedly called for saw-cut control joints placed at 15 ft. intervals, which reportedly appeared to be more like a 12 to 13 ft. spacing and 1.5 to 2 in. deep. Two cores, Nos. 1 and 3 were collected from areas that exhibit cracking and one core No. 2 was from a control area that seemed to be in better condition.

Field test reports showed slump varied from 6 to 7.5 in. and air content from 1.2 to 1.8 percent. Cylinder strength results provided later showed around 6000 psi strength at 28 days and in excess of 3500 psi strength in 7 days for a mix that is designed to have a 28-day compressive strength of 3500 psi (which was achieved by the laboratory cured cylinders within 7 days). Strength results of cylinders, therefore, showed a significant increase in strength (and hence, the modulus of elasticity) in 28-days, e.g., by as much as 170 percent, which could have increased the potential for unaccommodative drying shrinkage cracking of slab.

FIELD PHOTOGRAPHS

Figures 5 through 8 show locations of three cores in field photographs as well as visible cracking on the dense hard trowel-finished surface of slab that appeared to be continuous hairline cracks to network of fine crazy-type cracks on the surface. The hole left from removal of Core 1 showed extension of a surface crack to a depth of 2 inches. Core 3 shows almost a full-depth crack in its 6 in. length as well as numerous fine micro and macrocracking within the top 1 in. of surface. Area at the location of Core 2 did not show any visible cracking; however, the top near-surface region of Core 2 showed a small surface-parallel microcrack at a depth of 10 to 15 mm which is described later. Therefore, despite difference in appearance of visible cracking in the field, concrete in all three cores appeared to have undergone some micro to macrocracking at variable degrees – from low at the location of Core 2 to severe at the location of Core 3.

[redacted]

The following was performed in order to obtain 3 core samples from the floor slab on grade:

- MPM walked the interior slab with BB (Al Neyer) to discuss areas to be cored.
- Observations of shrinkage cracking in the slab including crazing was discussed.
- MPM observed two (2) definitive areas of concern where cracking was prominent. Cores were taken from each of these areas.
- A third core was taken from a location where minimal craze cracking was observed for use as a control sample.

Refer to the sketches below for approximate locations. The cores were then delivered to Construction Materials Consultants, Inc. (CMC) for chemical and petrographic analyses.

UNEXPECTED, UNUSUAL, OR NONCONFORMING OBSERVATIONS (NEW / RESOLVED)

The first core taken (#1) was estimated in the field to be less than 5 inches using a measuring tape. MPM showed BB the core, who in turn contacted Jim Doran for Doran construction regarding these observations.

SUMMARY OF MEETINGS / DISCUSSIONS / TELEPHONE CONVERSATIONS / VISITORS ONSITE

MPM discussed all observations made relevant to today's site visit with MGS.

ATTACHMENTS

Photos and sketch

DESCRIPTION OF SAMPLES TAKEN OR MATERIALS DELIVERED TO LAB

Three (3) concrete cores and delivered to CCE (lab)

*No representations or warranties are made regarding the accuracy of the information generated by the Theodolite application, which is stamped on the photo, or the suitability of that information for any; legal, engineering, surveying, or other use or purpose.

Figure 1: Daily field report received with the cores. Boxed area in the report stated observations on shrinkage cracking and crazing of the slab surface in two areas from where core samples were collected.

Approximate Location of Cores Received

[redacted]

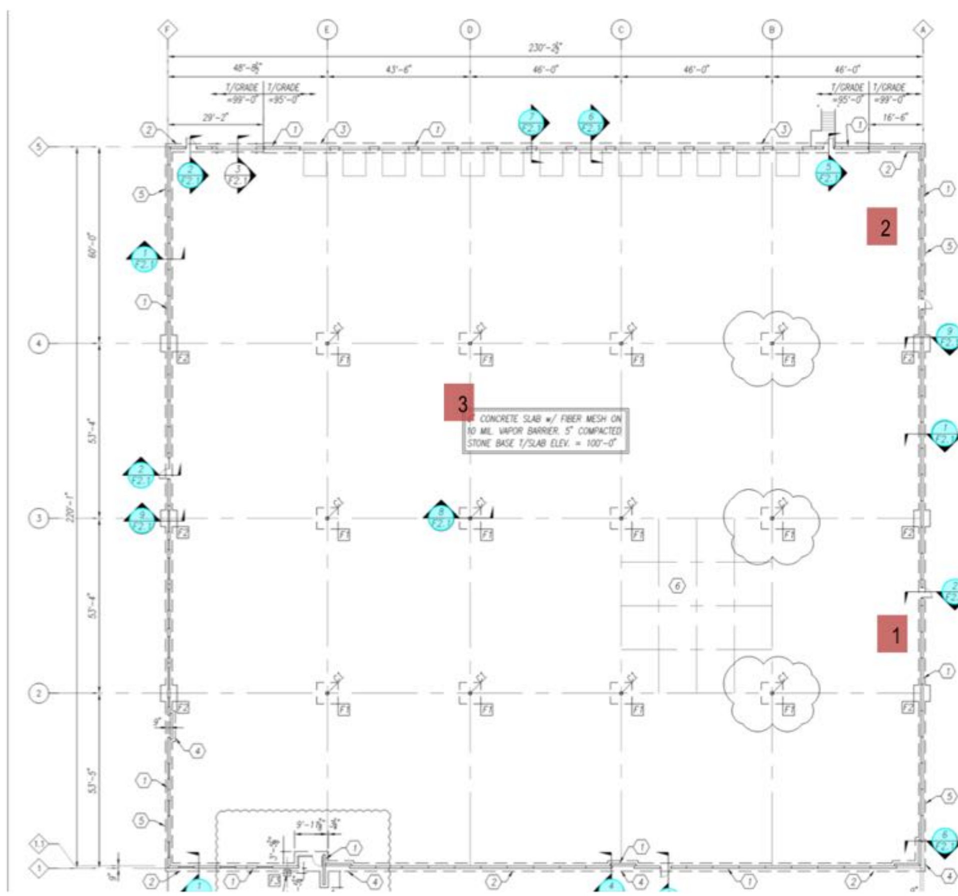

\# - Approximate location of cores taken.

1) 5-inch thick core
2) Control core (6 inches)
3) Core (6 inches)

*No representations or warranties are made regarding the accuracy of the information generated by the Theodolite application, which is stamped on the photo, or the suitability of that information for any; legal, engineering, surveying, or other use or purpose.

Figure 2: Drawing showing locations of three concrete cores received, of which Core Nos. 1 and 3 of respective 5-in. and 6-in. nominal thicknesses are from areas showing visible surface cracking, whereas Core No. 2 of nominal 6 in. thickness is from an area showing no visible cracking (control sample). All three cores were taken through full depths of slab at the locations hence indicating a variation in slab thickness from 5 to 6 inches.

Inspection Reports – Preparation Prior to Placement

[redacted]

INSPECTION REPORT

50° OVERNIGHT RAIN TO GRAY + BREEZY 60°

CLIENT: AL NEYER	REPORT NO.: 17
PROJECT: DON'S APPLIANCE II	JOB NUMBER: J-14666
LOCATION: CRAFTON, PA.	INSPECTOR: D.A. MEDICH
INSPECTION TYPE: SITE	DATE: 11-5-18 MONDAY.

1) EXCAVATED EXTERIOR FOOTER ON "A" LINE / "3.1" TO "5" LINE TO ON "5" LINE FROM "A" → NORTH 15'.

A) THE ABOVE SUBGRADE FOR FOOTER > 3000 PSF OF SURFACE BEARING CAPACITY ON COMPACTED SOILS.

2) LOCATION; INTERIOR COLUMN FOOTER # C4;

A) FULL OF RAIN WATER / PUMPED-OUT WATER.

B) UNDERCUT ADDITIONAL 18" DEPTH TO REMOVE MUD AND SATURATED SOILS TO > 3000 PSF SURFACE BEARING CAPACITY ON COMPACTED SOILS.

C) BACKFILLED UNDERCUT WITH #2A LIMESTONE, PLACED IN 6" LIFTS, AND THOROUGHLY COMPACTED WITH VIBRATORY "HOE-PAC" TO NON-MOVEMENT AND A MINIMUM OF 95% D1557 COMPACTION AS SPECIFIED.

* SEE IN-PLACE DENSITY REPORT FOR COMPACTION RESULTS.

3) PLACED 43 1/2 C.Y. OF 3000 PSI CONCRETE AS FOLLOWS; LOCATION; FTRS. ON "A" / "3.1" TO "5" / THEN ON 5 TO 15' → NORTH

A) PERFORMED SLUMP, AIR-CONTENT, TEMPERATURE AND CAST CYLINDERS # DA-08 FOR COMPRESSIVE STRENGTH TESTING.

B) REINFORCING STEEL INSTALLED AS PER DRAWINGS.

[redacted]

INSPECTION REPORT

50° LT. RAIN TO SUN + 35 MPH WINDS

CLIENT: AL NEYER	REPORT NO.: 18
PROJECT: DON'S APPLIANCE II	JOB NUMBER: J-14666
LOCATION: CRAFTON, PA.	INSPECTOR: D.A. MEDICH
INSPECTION TYPE: SITE	DATE: 11-6-18 TUESDAY

1) CONTRACTOR IS "DE-MUCKING" ENTIRE INTERIOR BUILDING SLAB-ON-GRADE AS FOLLOWS;

A) REMOVING WATER AND SATURATED SOILS.

B) AERATING TO DRY WITH 30 TO 35 MPH SUSTAINED WINDS.

C) SCHEDULED TO PROOFROLL TOMORROW 11-7-18 WEDNESDAY.

[redacted]

INSPECTION REPORT

45° TO 52° SUN + WINDY (14 TO 22 MPH)

CLIENT: AL NEYER	REPORT NO.: 19
PROJECT: DON'S APPLIANCE II	JOB NUMBER: J-14666
LOCATION: CRAFTON, PA	INSPECTOR: D.A. MEDICH
INSPECTION TYPE: SITE	DATE: 11-7-18 WEDNESDAY

1) PROOFROLLED SUBGRADE SOILS AS FOLLOWS;

LOCATION; INTERIOR BUILDING SLAB-ON-GRADE SUBGRADE SOILS. "A" TO "F" LINES / "1" TO "4.8" LINES.
* NOTE; "4.8" TO "5" LINES WILL BE EXCAVATED FOR LOADING DOCKS

A) PROOFROLLED WITH 13 TON VIBRATORY ROLLER TO NON-MOVEMENT WHILE THOROUGHLY COMPACTING. = SATISFACTORY.

B) BEGAN PLACING #2A CRUSHED CONCRETE SUBBASE STONE.

C) PERFORMED IN-PLACE DENSITY TESTS TO VERIFY "ACCEPTABLE" MOISTURE CONTENT OF #2A SUBBASE STONE.

** NOTE: LOC; "A" TO "B.5" / "1" TO "2" LINE.
1) REMOVED PREVIOUSLY PLACED, SATURATED SUBBASE STONE AND UNDERCUT SUBGRADE SOILS TO SOLID. AND PROOFROLLED TO NON-MOVEMENT.

[redacted]

INSPECTION REPORT

32° SUN TO 45° PARTLY CLOUDY

CLIENT: AL NEYER	REPORT NO.: 20
PROJECT: DON'S APPLIANCE II	JOB NUMBER: J-14666
LOCATION: CRAFTON, PA.	INSPECTOR: D.A. MEDICH
INSPECTION TYPE: SITE	DATE: 11-8-18 THURSDAY

1) LOCATION; "A" TO "B" / "1" TO "2" LINES. (UNDERCUT YESTERDAY). SOUTHWEST CORNER.

A) PLACED 6" TO 8" LIFT OF #4 STONE AND THOROUGHLY COMPACTED WITH LARGE (13 TON) VIBRATORY SMOOTH DRUM ROLLER TO NON-MOVEMENT.

2) LOCATION; ENTIRE BLDG. AREA "A" TO "E" / "1" TO "4.8" LINE SUBBASE STONE.

A) PLACED SUBBASE STONE AND LASER GRADED AND THOROUGHLY COMPACTED TO NON-MOVEMENT WITH LARGE VIBRATORY ROLLER AND A MINIMUM OF 95% D1557 COMPACTION AS SPECIFIED.

* SEE IN-PLACE DENSITY REPORT FOR COMPACTION TEST RESULTS.

3) INSTALLING PERIMETER INSULATION BOARD AS PER DRAWINGS ON "1" LINE AND "E" LINE.

Figure 3: Reports of field inspection during placement of concrete slab, received with the cores.

Inspection Reports & Field Testing Data – During Placement

[redacted]

INSPECTION REPORT

CLIENT: Al Neyer	REPORT NO.: 21
PROJECT: Don's Appliance II	JOB NUMBER: 14666
LOCATION: Pittsburgh, PA	INSPECTOR: M. Graham
INSPECTION TYPE: Concrete	DATE: 11/10/18

Approx. 450 Total cubic yards of a 3500psi Non-Air entrained concrete mix with 2% Non-chloride, Fiber, and Super added was used by Doran to place interior S.O.G. Pour #1. Five sets of concrete tests were taken which consist of Slump, Temperature, and Air Content. Also (25) 4x8in cylinders were cast for compressive strength testing. All testing passed in accordance with job specifications. Vapor Barrier was all installed and properly taped prior to concrete placement. See breaksheets for Results.

[redacted]

CONCRETE FIELD TESTING DATA SHEET

DATE: 11/10/18 | CLIENT: AL Neyer | REPORT NO.:
PROJECT: Don's Appliance's II | JOB NUMBER: 14666
POUR LOCATION: Interior S.O.G. Pour #
CONCRETE CLASS: 3500 Non-Air; Fiber; 2% Non-Chloride; Super

CU. YDS.	TIME	TRUCK NO.	TICKET NO.	SLUMP (in.)	AIR CONT. (%)	CON. TEMP. (F)	DENSITY (lbs/ft³)	TEST SET NO.'S	NOTES
10	12:55am	1416	18032	6½in	1.2%	72°F	–	DA-A	–
110	1:15am	4104	18042	7in	1.6%	76°F	–	B	–
210	2:00am	4103	18052	7in	1.3%	71°F	–	C	–
310	3:25am	146	18062	7½in	1.4%	70°F	–	D	–
340	4:35am	4106	18065	6in	1.8%	76°F	–		–

Placement Date – November 10, 2018
Slump: 6.5-7 in. Air: 1.2-1.8%

REMARKS: Total of 440 cubic yds placed

APPLICABLE TEST PROCEDURES (U.N.O.)
Sampling: ASTM C172
Slump: ASTM C143
Air Content: ASTM C231 or ASTM C173
Temperature: ASTM C1064
Density: ASTM C138
Casting Specimens: ASTM C31

SPEC. REQ'TS:
SLUMP: 8in±1½ TEMP: 60°-80°F
AIR: Non-Air DENSITY:
w/Super P Added

M. Graham
TECHNICIAN

REVIEWER DATE 11/19/18

[redacted]

INSPECTION REPORT

CLIENT: Al Neyer	REPORT NO.: 22
PROJECT: Don's Appliance's II	JOB NUMBER: 14666
LOCATION: Pittsburgh, PA	INSPECTOR: M. Graham
INSPECTION TYPE: Concrete	DATE: 11/11/18

Approx. 340 Total cubic yards of a 3500psi Non-Air entrained concrete mix with 2% Non-chloride, Fiber, and Super added was used by Doran to place interior S.O.G. Pour #2. Four sets of concrete tests were taken which consist of Slump, Temperature, and Air Content. Also (20) 4x8in cylinders were cast for compressive strength testing. All testing passed in accordance with job specifications. Vapor Barrier was all installed and properly taped prior to concrete placement. See breaksheets for Results.

[redacted]

CONCRETE FIELD TESTING DATA SHEET

DATE: 11/11/18 | CLIENT: AL Neyer | REPORT NO.:
PROJECT: Don's Appliance's II | JOB NUMBER: 14666
POUR LOCATION: Interior S.O.G. Pour #
CONCRETE CLASS: 3500 Non-Air; Fiber; 2% Non-Chloride; Super

CU. YDS.	TIME	TRUCK NO.	TICKET NO.	SLUMP (in.)	AIR CONT. (%)	CON. TEMP. (F)	DENSITY (lbs/ft³)	TEST SET NO.'S	NOTES
10	12:50am	164	18078	6in	1.4%	71°F	–	DA-A	–
110	2:00am	113	18088	7in	1.6%	70°F	–	B	–
210	3:15am	160	18098	7½in	1.4%	71°F	–	C	–
310	5:00am	153	18105	7in	1.2%	73°F	–	D	–

Placement Date – November 11, 2018
Slump: 6-7.5 in. Air: 1.2-1.6%

REMARKS: Approx. 340 Total cubic yards placed.

APPLICABLE TEST PROCEDURES (U.N.O.)
Sampling: ASTM C172
Slump: ASTM C143
Air Content: ASTM C231 or ASTM C173
Temperature: ASTM C1064
Density: ASTM C138
Casting Specimens: ASTM C31

SPEC. REQ'TS:
SLUMP: 8in±1½ TEMP: 60°-80°F
AIR: Non-Air DENSITY:
w/Super P Added

M. Graham
TECHNICIAN

REVIEWER DATE 11/19/18

Figure 4: Reports of field inspection during placement of concrete slab, received with the cores. Notice two placement dates on November 10 and 11 of 2018 with respective 6 to 7.5 in. slump, and air contents of 1.2 to 1.8 percent of freshly placed concrete on both dates.

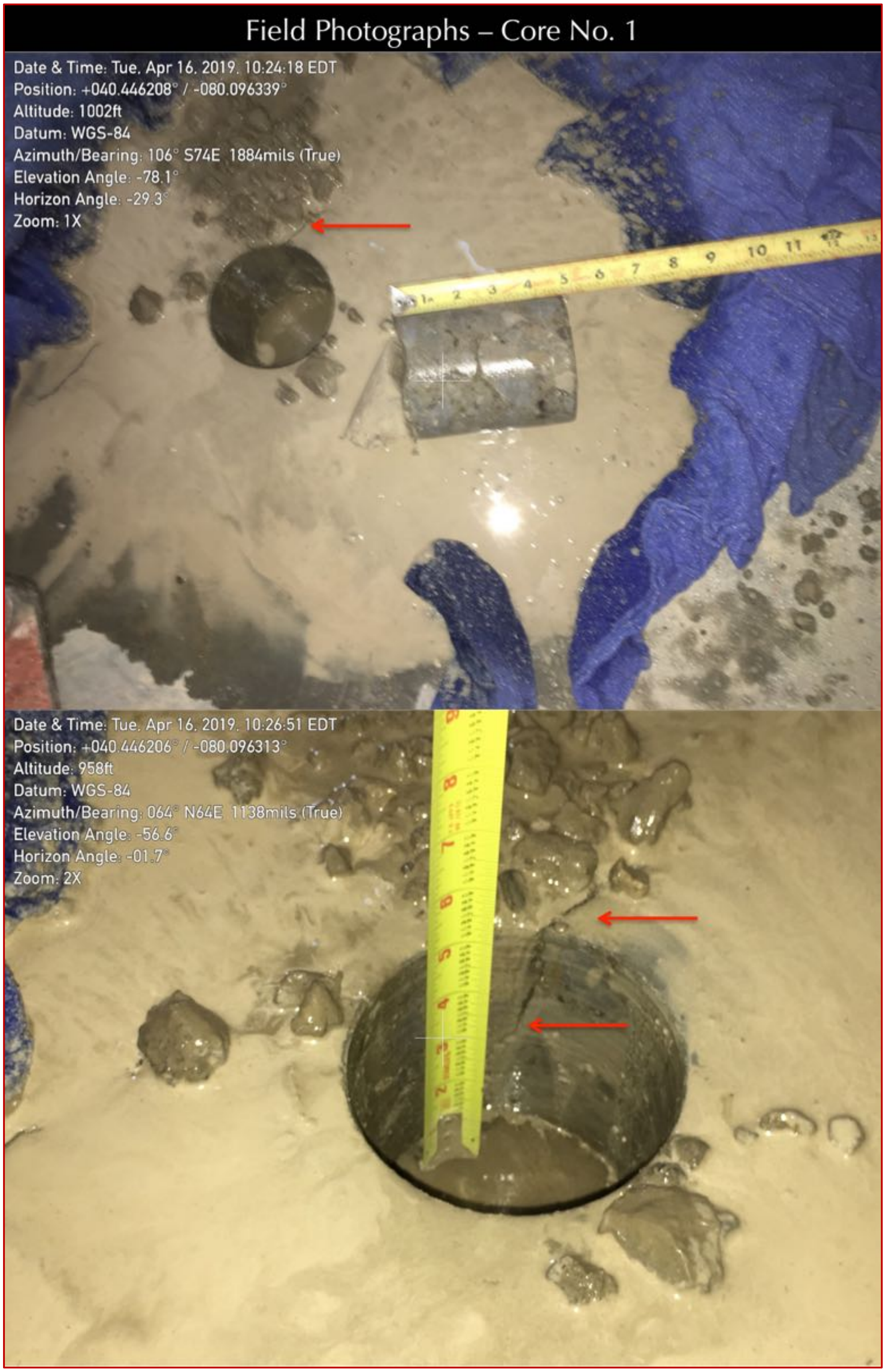

Figure 5: Field photographs showing retrieval of Core 1 from an area where slab showed fine hairline craze-type surface cracking on the smooth, flat, dense, hard trowel-finished surface. Core 1 is 5 in. in nominal length, drilled through full-depth of the slab. Notice extension of surface crack (arrows) through depth at the wall of the hole formed after removal of core in the bottom photo.

Field Photographs – Core No. 2

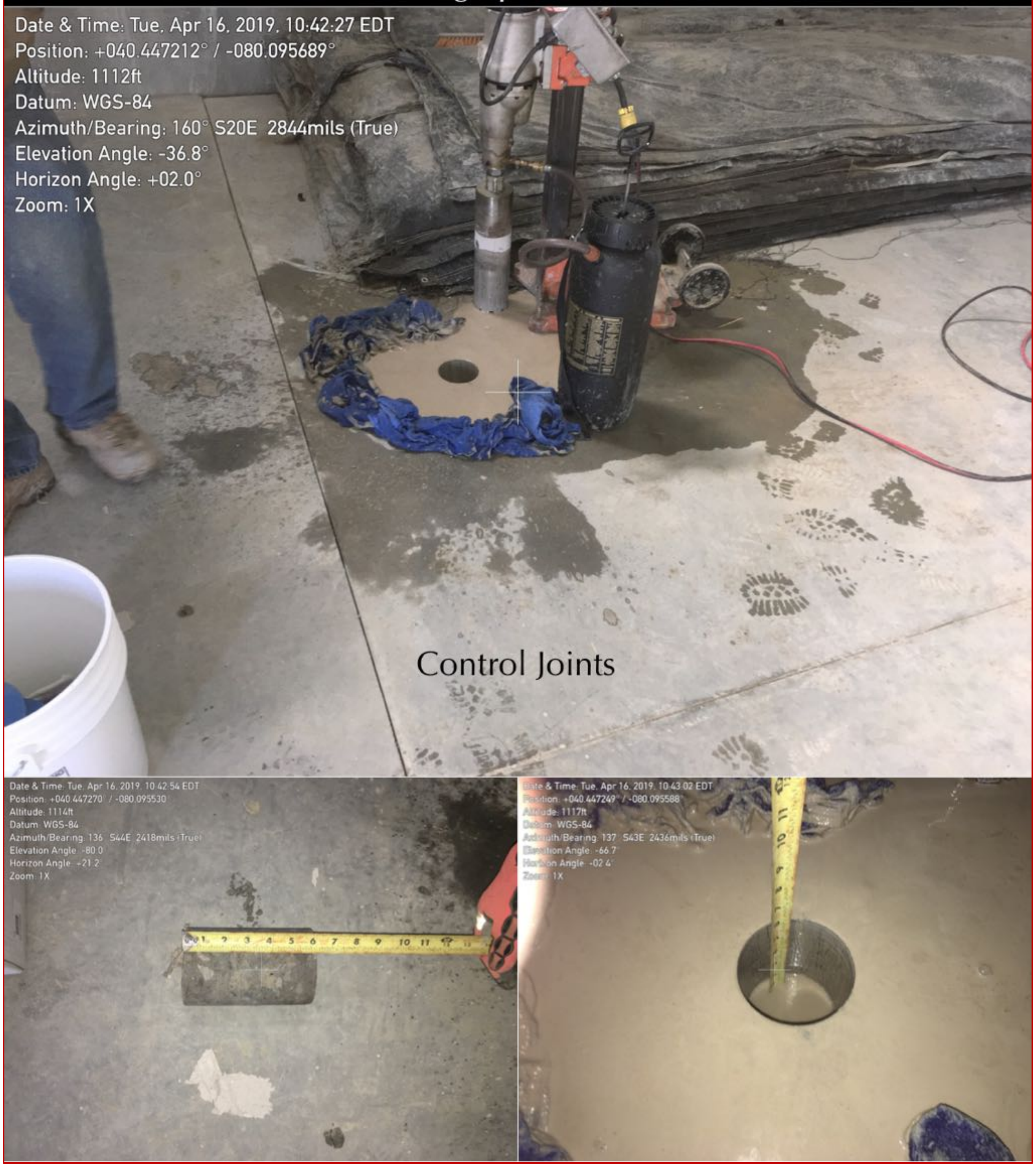

Figure 6: Field photographs showing retrieval of Core 2 from an area where slab showed no visible surface cracking, and a smooth, flat, dense, hard trowel-finished surface. Core 2 is 6 in. in nominal length, drilled through full-depth of the slab.

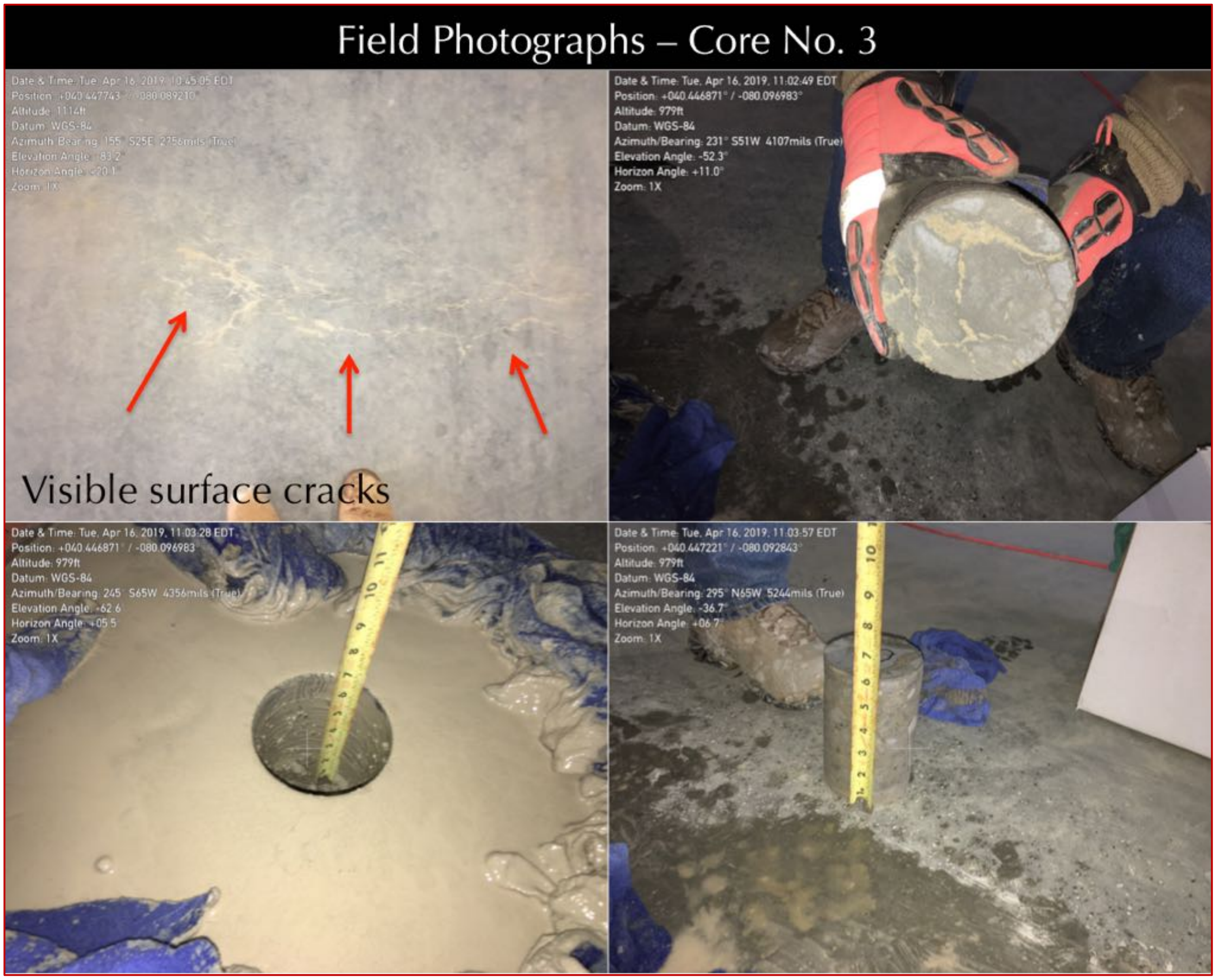

Figure 7: Field photographs showing retrieval of Core 3 from an area where slab showed fine hairline craze-type surface cracking on the smooth, flat, dense, hard trowel-finished surface. Core 3 is 5 in. in nominal length, drilled through full-depth of the slab. Visible cracks on the slab surface at the location of core are shown in the top left photo, whereas some of those cracks on the core top surface after removal are shown in the top right photo.

PURPOSE OF PRESENT INVESTIGATION

Based on the background information provided, the purposes of the present investigation are to determine:

a. The composition, quality, and overall condition of concrete in the cores;
b. Evidence of any physical or chemical deterioration of concrete in the cores; and,
c. Based on detailed laboratory investigation, investigation of all possible reasons to explain the observed and reported surface cracking of concrete slab.

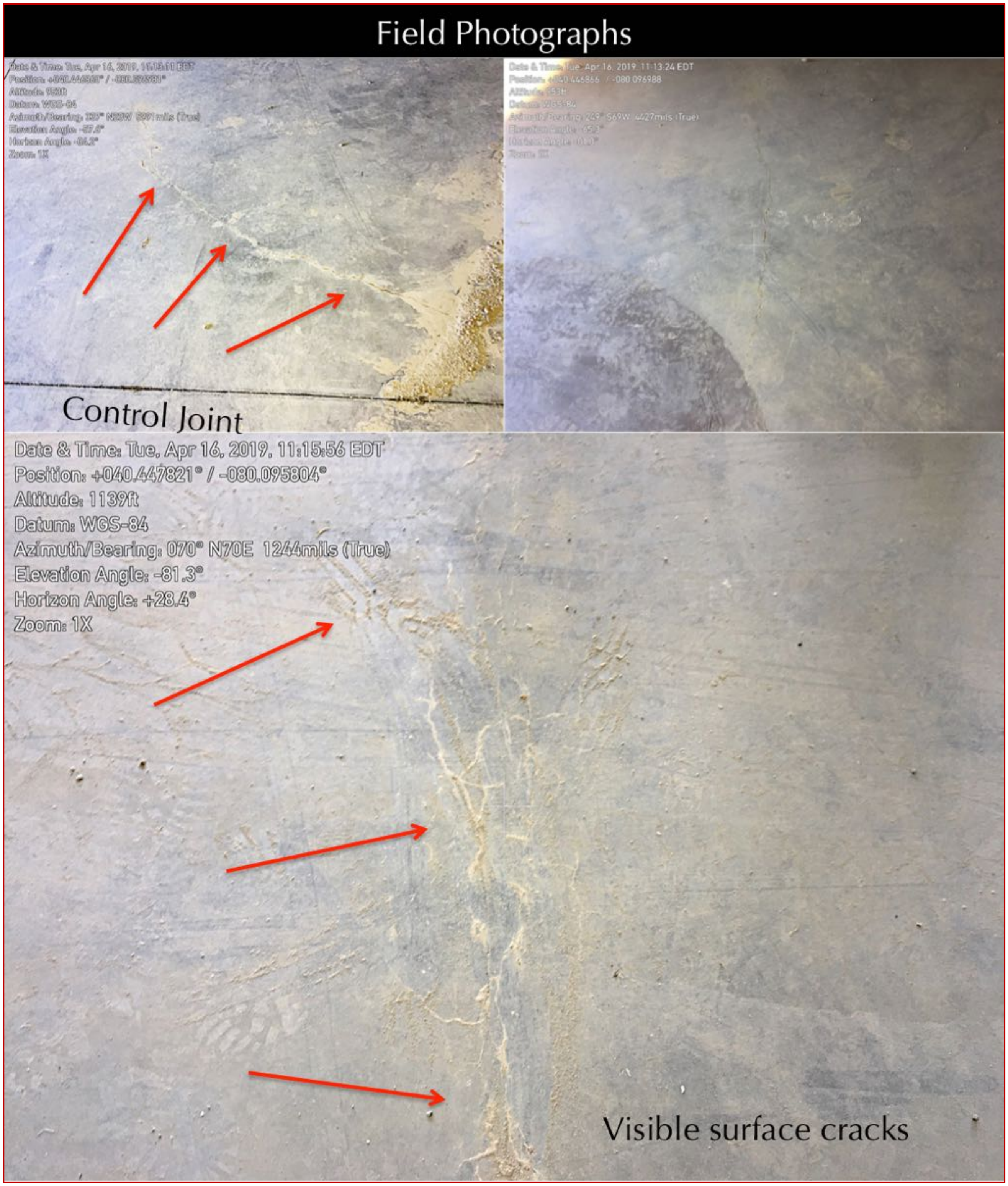

Figure 8: Field photograph showing overall smooth, flat, dense, hard, dark gray slab surface and occurrences of long, continuous fine visible cracks marked with arrows. Notice a control joint in the top left photo.

SAMPLES

PHOTOGRAPHS, IDENTIFICATION, INTEGRITY, AND DIMENSIONS

Figures 9 to 11 show the three cores as received. The cores have nominal diameters of 4 in. (100 mm) for Nos. 1, 2, and 3 and respective nominal lengths of 5 in. (125 mm), 6 in. and 6 in. (150 mm).

END SURFACES

All three cores showed a smooth flat, dense, dark gray hard burned steel trowel finished top surface representing the trowel-finished surface of slab, and, a formed wavy bottom surface with adhered remains of fiberglass reinforced plastic vapor retarder indicating placement of the slab on a vapor retarder.

CRACKING & OTHER VISIBLE DISTRESS, IF ANY

Core 1 showed a major visible crack at one edge that has extended to a depth of 2 inches. Core 3 showed almost full-depth cracking appeared as fine hairline cracks as well as network of craze cracking on the top surface. By contrast, top surface and side of Core 2 showed no visible cracking.

EMBEDDED ITEMS

Distributed throughout the concrete in all three cores are fine, hair like polypropylene-type synthetic fibers that are consistent with the reported use of a fiber-reinforced concrete in the slab. No reinforcing steel, wire mesh, or other embedded items are present in the cores.

RESONANCE

The cores have a ringing resonance, when hammered.

TESTING STRATEGY

Each core was tested for detailed petrographic examinations and chemical profiles from the top finished surface region, mid-depth location, and bottom end. Details of testing methodologies are provided in the next section. Each core was sectioned longitudinally into multiple slabs with oil-cooled diamond saw. A sectioned slab was then lapped with successively finer diamond abrasives in metal and resin-bonded diamond lapping discs with water used as coolant. Additional sectioned slab was used to prepare blue dye-mixed epoxy-impregnated thin sections of concrete from the top 2 inches of each core. Finally, chemical profiles for water-soluble anions (chloride, nitrate, sulfate), and cations (sodium, potassium, calcium) were determined from the top, mid-depth, and bottom ends of each core.

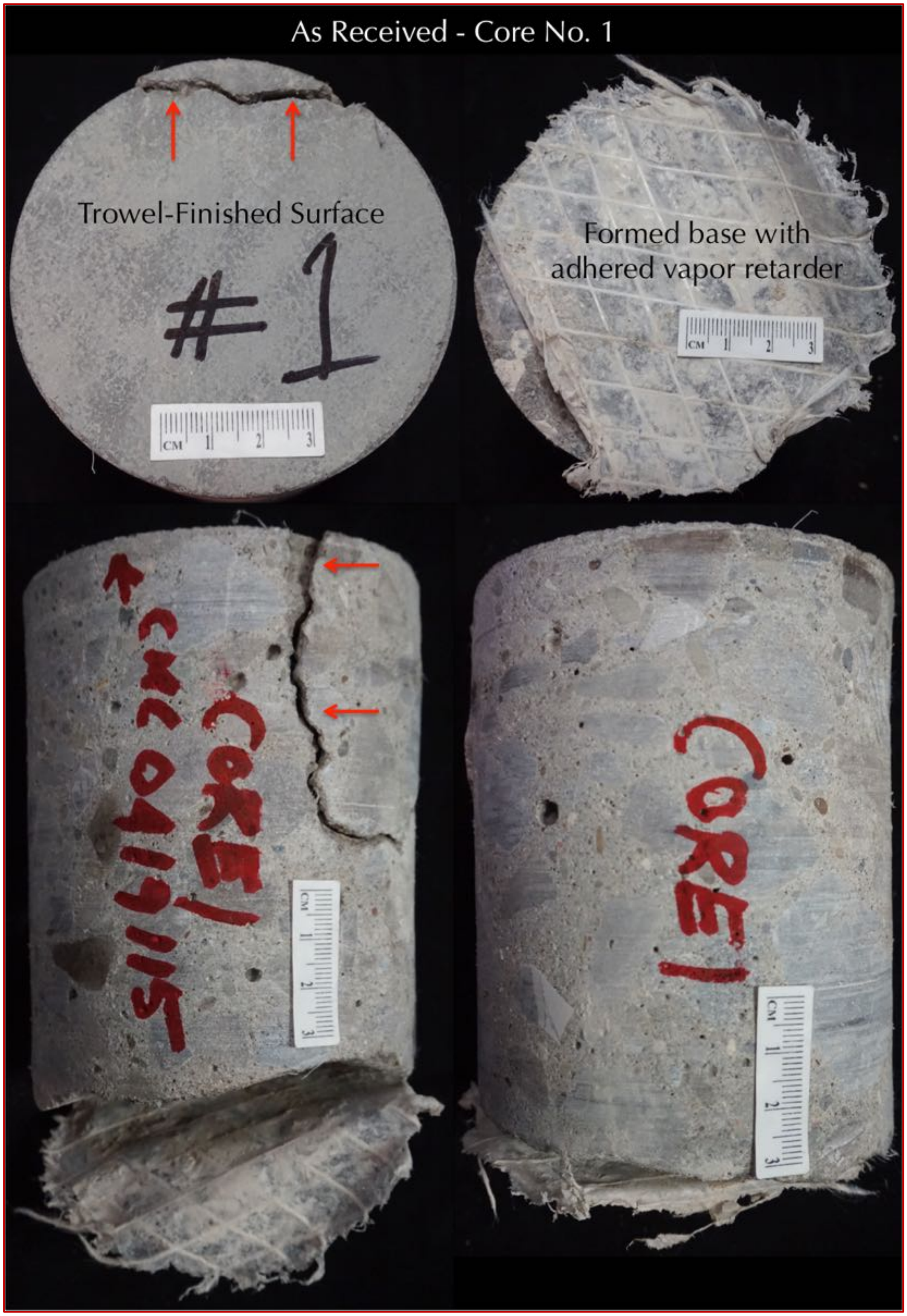

Figure 9: Photos of Core 1 as received. Top left – Top end of core showing smooth, flat, dense, hard, dark gray, trowel-finished surface of slab on which is a visible crack (arrows) that was probably widened during coring and core retrieval processes. Top right – Bottom end of core showing wavy, formed bottom surface of slab with remains of a fiber-reinforced plastic vapor retarder on which the slab was placed. Bottom row – Side views of the core showing partial-depth extension of the surface crack to a depth of about 2 inches, and overall dense, well-consolidated nature of concrete away of the visible crack.

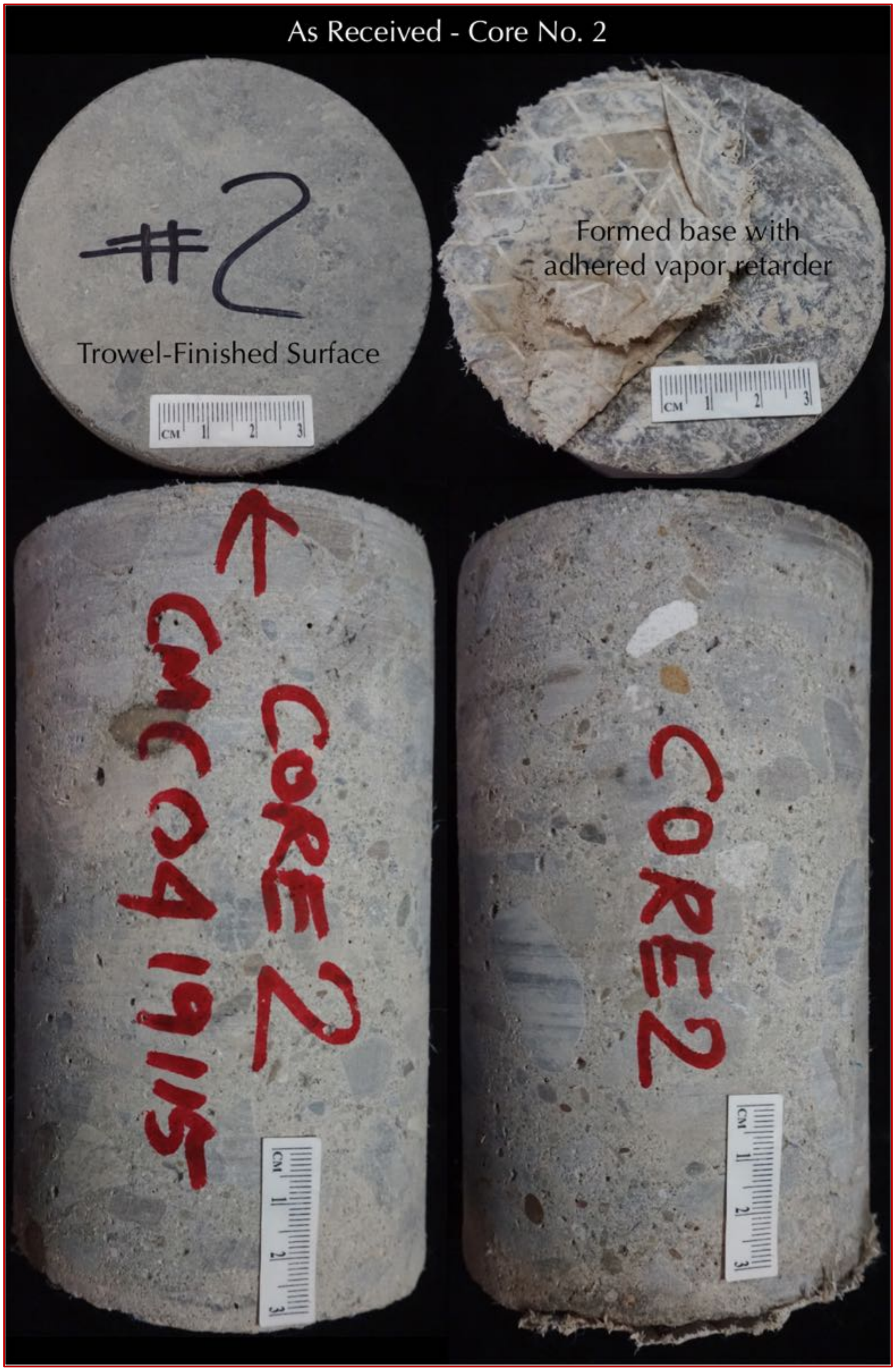

Figure 10: Photos of Core 2 as received. Top left – Top end of core showing smooth, flat, dense, hard, dark gray, trowel-finished surface of slab with no visible cracking. Top right – Bottom end of core showing wavy, formed bottom surface of slab with remains of a fiber-reinforced plastic vapor retarder on which the slab was placed. Bottom row – Side views of the core showing overall dense, well-consolidated nature of concrete.

Figure 11: Photos of Core 3 as received. Top left – Top end of core showing smooth, flat, dense, hard, dark gray, trowel-finished surface of slab on which is a network of visible cracks (arrows) similar to fine, hairline craze cracking. Top right – Bottom end of core showing wavy, formed bottom surface of slab with remains of a fiber-reinforced plastic vapor retarder (not shown in the photo but received with the core) on which the slab was placed. Bottom row – Side views of the core showing almost full-depth extension of the surface cracks (arrows), and overall dense, well-consolidated nature of concrete away of the visible cracks.

METHODOLOGIES

PETROGRAPHIC EXAMINATIONS

The cores were examined by petrographic examinations by following the methods of ASTM C 856 "Standard Practice for Petrographic Examination of Hardened Concrete." Details of petrographic examinations and sample preparation are described in Jana (1997a, b, 2001, 2004a, b, 2005a, b, 2006, 2007).

The steps of petrographic examinations include (Jana 2006):

i. Visual examinations of samples, as received;
ii. Low-power stereomicroscopical examinations of as-received, saw-cut and freshly fractured sections, and lapped cross sections of cores for evaluation of textures, and composition;
iii. Low-power stereomicroscopical examinations of air contents and air-void systems of concrete in the cores;
iv. Examinations of oil immersion mounts in a petrographic microscope for mineralogical compositions of specific areas of interest;
v. Examinations of blue dye-mixed (to highlight open spaces, cracks, etc.) epoxy-impregnated large area (50 mm × 75 mm) thin sections of concrete in a petrographic microscope for detailed compositional and microstructural analyses;
vi. Photographing samples, as received and at various stages of preparation with a digital camera and a flatbed scanner;
vii. Photomicrographs of lapped section and thin section of samples taken from stereomicroscope and petrographic microscope, respectively to provide detailed compositional and mineralogical information of concrete.

Figure 12: Nikon Eclipse E600POL Petrographic Microscope with Jenoptik Gryphax Camera (left), Olympus SZH (middle), and Nikon SMZ-10A Stereomicroscope (right) used for petrographic examinations.

CHEMICAL PROFILES

Profiles of water-soluble ions from the top, mid-depth, and bottom locations of cores were done by: (a) potentiometric titration, for water-soluble chloride contents *a la* ASTM C 1218 by using Metrohm 751 DMS Titrino with attached 730 Auto Sample Processor (Figure 13), (b) anion chromatography, *a la* ASTM D 4327 for water-soluble fluoride, chloride, nitrate, nitrite, bromide, phosphate, and sulfate ions by using Metrohm 881 Compact IC Professional with attached 858 Professional Sample Processor (Figure 13) with a sodium carbonate-bicarbonate eluent, and (c) cation chromatography for water-soluble alkalis (sodium, potassium), and calcium ions by using Metrohm 861 Advanced Compact IC with attached 788 IC Sample Processor (Figure 13) with nitric acid/dipicolinic acid eluent.

For all these tests, a representative portion of concrete from top, mid-depth, and bottom end of each core was sectioned and pulverized to fine powders passing US No. 20 sieve. About 10±0.01 gm. of powder sample was dispersed with 50-mL deionized water in a 250-mL beaker; stirring and breaking up any lumps with a glass rod, covered with a watch glass, and further stirred in a magnetic stirrer. The covered mixture in the beaker was then heated rapidly to boiling, but not more than a few seconds, then removed from hot plate, cooled down to room temperature, kept for further digestion for 24 hours while continuously stirring with magnetic stirrer preventing any evaporation with the covered watch glass. The digested sample solution was then filtered under vacuum, first through two 2.5-micron filter papers, followed by another filtration through two 0.2 micron filter papers to collect the filtrate. The filtrate thus obtained was diluted to a final volume of 200 ml in a volumetric flask.

About 50 mL from the final 200-mL filtrate was taken for ion chromatography. To the rest 150-mL filtrate to be used for potentiometric titration, a 3 mL of H_2O_2 (30%) and another 3 mL of HNO3 (1:1) were added, then heated rapidly to boiling but not more than a few seconds by removing from hot plate, cooled down to room temperature and used for titration for chloride content.

Metrohm equipments used for potentiometric titration and ion chromatography are all calibrated with known solutions, e.g., an 0.05N NaCl solution in 150-mL deionized water to run first for chloride titration, at least 7 to 10 standards of concentrations from 1-ppm to 100-ppm range to run for anion chromatography, and five standards from 2-ppm to 100-ppm range to run for cation chromatography.

Final results in terms of weight percent chloride by mass of concrete to the nearest 0.001% is determined for Cl, % = 3.545 [(V1-V2)N]/W, where V1 = milliliters of 0.05 N $AgNO_3$ solution used for sample titration (equivalent point), V2 = Milliliters of 0.05N $AgNO_3$ solution used for blank titration (equivalent point); N = exact normality of 0.05 N $AgNO_3$ solution, and W = mass of sample in grams. This equation is equivalent to % chloride = (equivalent point from titration times 0.177) divided by sample weight in grams.

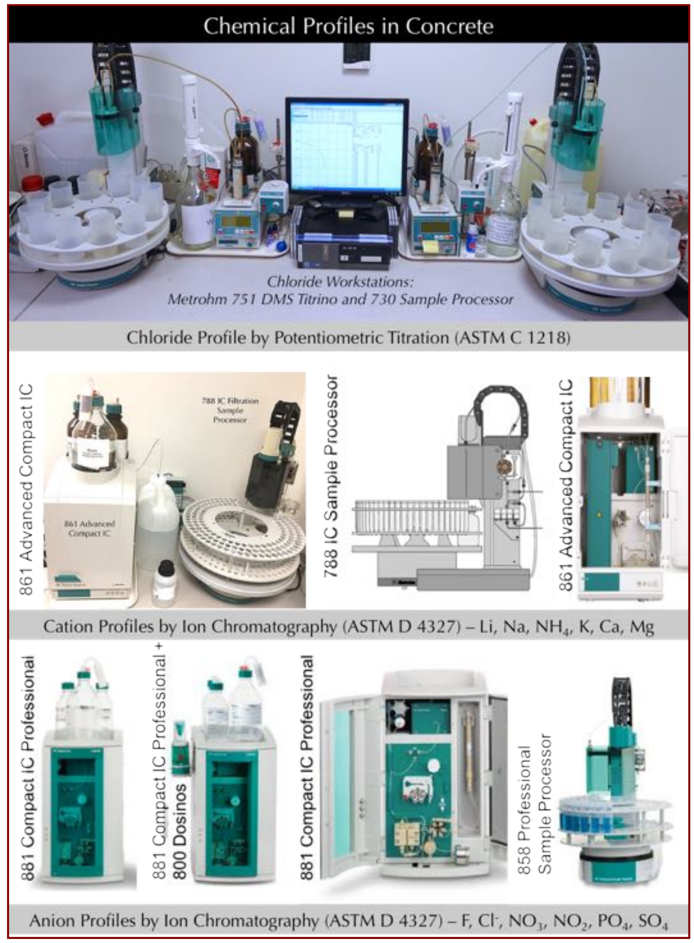

Figure 13: Top: Potentiometric titration for water-soluble chloride contents (ASTM C 1218) with Metrohm 751 DMS Titrino, 730 Sample Processor, and Tiamo software. Middle – Ion chromatography of water-soluble cations with Metrohm 861 Advanced Compact IC with 788 Sample Processor, and MagIC Net software. Bottom – Ion Chromatography of water-soluble anions with Metrohm 881 Compact IC Professional with 858 Sample Processor and MagIC Net software.

Final results of ion chromatography in terms of weight percent ions by mass of concrete are obtained from: [(ppm-concentrations from IC (which include appropriate dilution factors) × original filtrate volume (200 mL)] ÷ [(Sample weight, 10±0.01 gm) × (10,000 to for conversion of ppm to wt. percent)].

Figure 14: Saw-cut sections of cores showing testing strategies on each saw-cut section – from (a) preparation of lapped cross section, to (b) a saw-cut section treated with phenolphthalein alcoholic solutions to determine the depth of carbonation of concrete, to (c) preparation of a trimmed section for blue dye-mixed epoxy impregnation for thin section, to (d) further sectioning of a top, mid-depth, and bottom end of the core for determination of water-soluble chloride, sulfate and other chemical profiles from the slab.

PETROGRAPHIC EXAMINATIONS

LAPPED CROSS SECTIONS

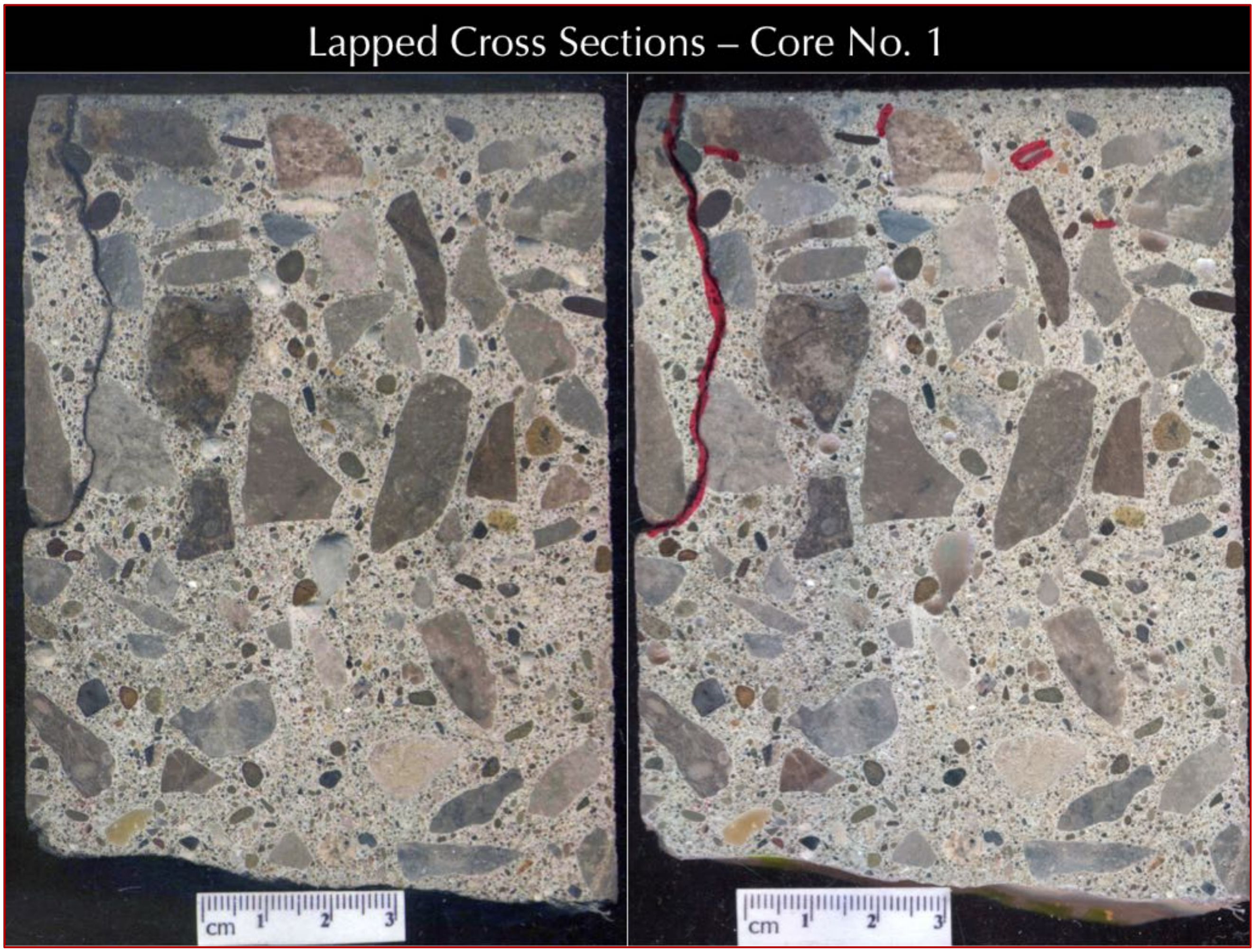

Figure 15: Lapped cross section of Core 1 showing: (a) crushed limestone-dolomite coarse aggregate, natural siliceous-calcareous sand fine aggregate, and well-graded, and well-distributed coarse and fine aggregates, (b) dense and well-consolidated nature of concrete, (c) densified finished surface region at the very top near-surface region (where paste is denser and darker gray than the body) due to trowel-finishing operations, (d) uniform color tone of paste in the body, except for the darker gray paste at the very top from trowel-finishing, and (e) partial-depth extension of the surface crack at the edge of the core to a depth of about 2 inches. The main crack and small short discontinuous separations at the top 1 in. of the finished surface region are highlighted in red in the right photo.

Figure 16: Lapped cross section of Core 2 showing: (a) crushed limestone-dolomite coarse aggregate, natural siliceous-calcareous sand fine aggregate, which are compositionally similar to the ones found in the concrete in Core 1, and well-graded, and well-distributed coarse and fine aggregates, (b) dense and well-consolidated nature of concrete, (c) densified finished surface region at the very top near-surface region (where paste is denser and darker gray than the body) due to trowel-finishing operations, (d) uniform color tone of paste in the body, except for the darker gray paste at the very top from trowel-finishing, and (e) occurrence of a few fine, hair-like microcracking at the near-surface region of concrete to a depth of 10 to 15 mm from the finished surface, which is highlighted in red line in the right photo. Therefore, despite the absence of any visible macro or microcracks at the top finished surface at this core location, however, the interior concrete beneath the surface showed some microcracking at a depth of 10 to 15 mm from the finished surface.

Figure 17: Lapped cross section of Core 3 showing: (a) crushed limestone-dolomite coarse aggregate, natural siliceous-calcareous sand fine aggregate, which are compositionally similar to the ones found in the concrete in Cores 1 and 2, and well-graded, and well-distributed coarse and fine aggregates, (b) dense and well-consolidated nature of concrete, (c) densified finished surface region at the very top near-surface region (where paste is denser and darker gray than the body) due to trowel-finishing operations, (d) uniform color tone of paste in the body, except for the darker gray paste at the very top from trowel-finishing, and (e) extensive fine, hair-like micro and macro cracking at the top 1 in. of the finished surface as well as vertical almost full-depth cracking that are highlighted in red in the right photo. Of the three cores received, Core 3 showed maximum cracking both at the top 1 in. of the finished surface region as well as through depth.

SAW-CUT SECTIONS TREATED WITH PHENOLPHTHALEIN ALCOHOLIC SOLUTUIONS TO DETERMINE DEPTH OF CARBONATION OF CONCRETE

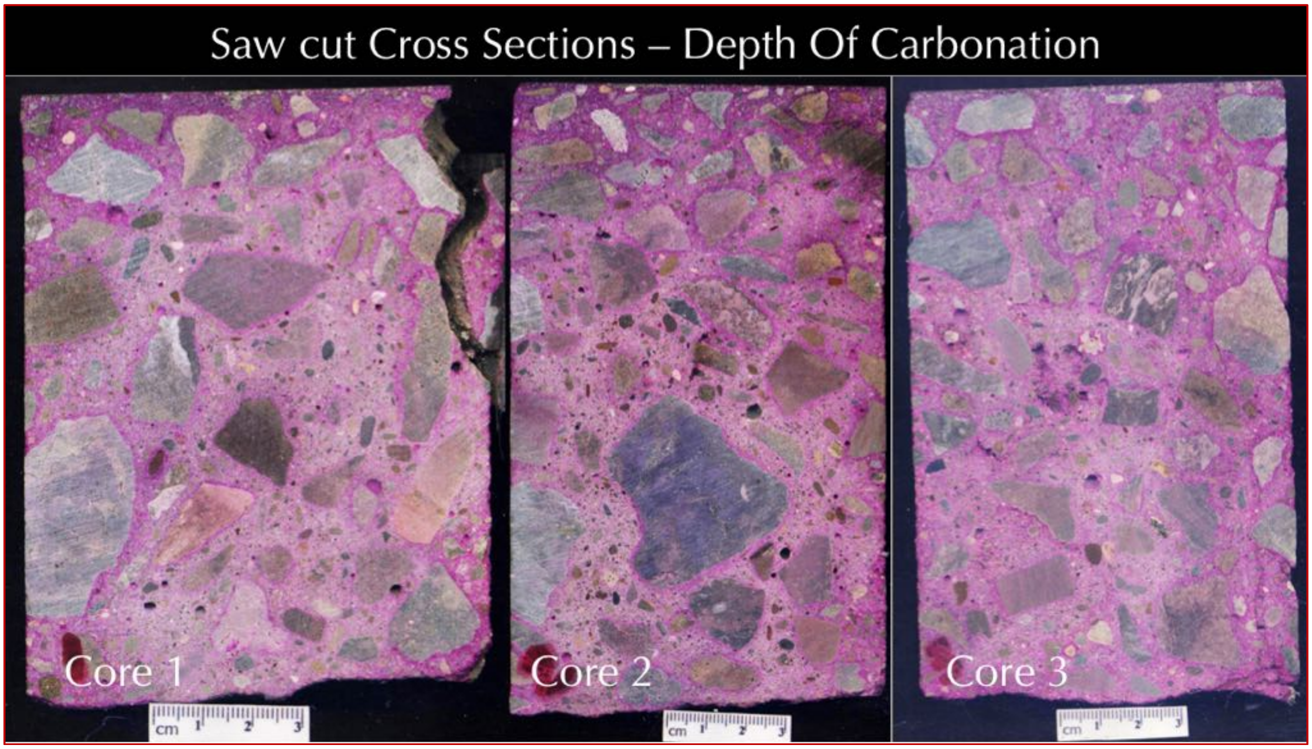

Figure 18: Saw-cut sections of cores treated with phenolphthalein alcoholic solutions showing depth of carbonation of concrete. Notice the absence of any carbonation of paste where paste would have turned normal gray color tone of paste (which is present only as a thin layer at the very top was found in subsequent examinations of thin sections in a petrographic microscope but are difficult to find in these saw-cut sections). Concrete is non-carbonation beneath the finished surfaces hence turned to pink discolored sections.

FLUORESCENT DYE-MIXED EPOXY IMPREGNATED LAPPED CROSS SECTIONS

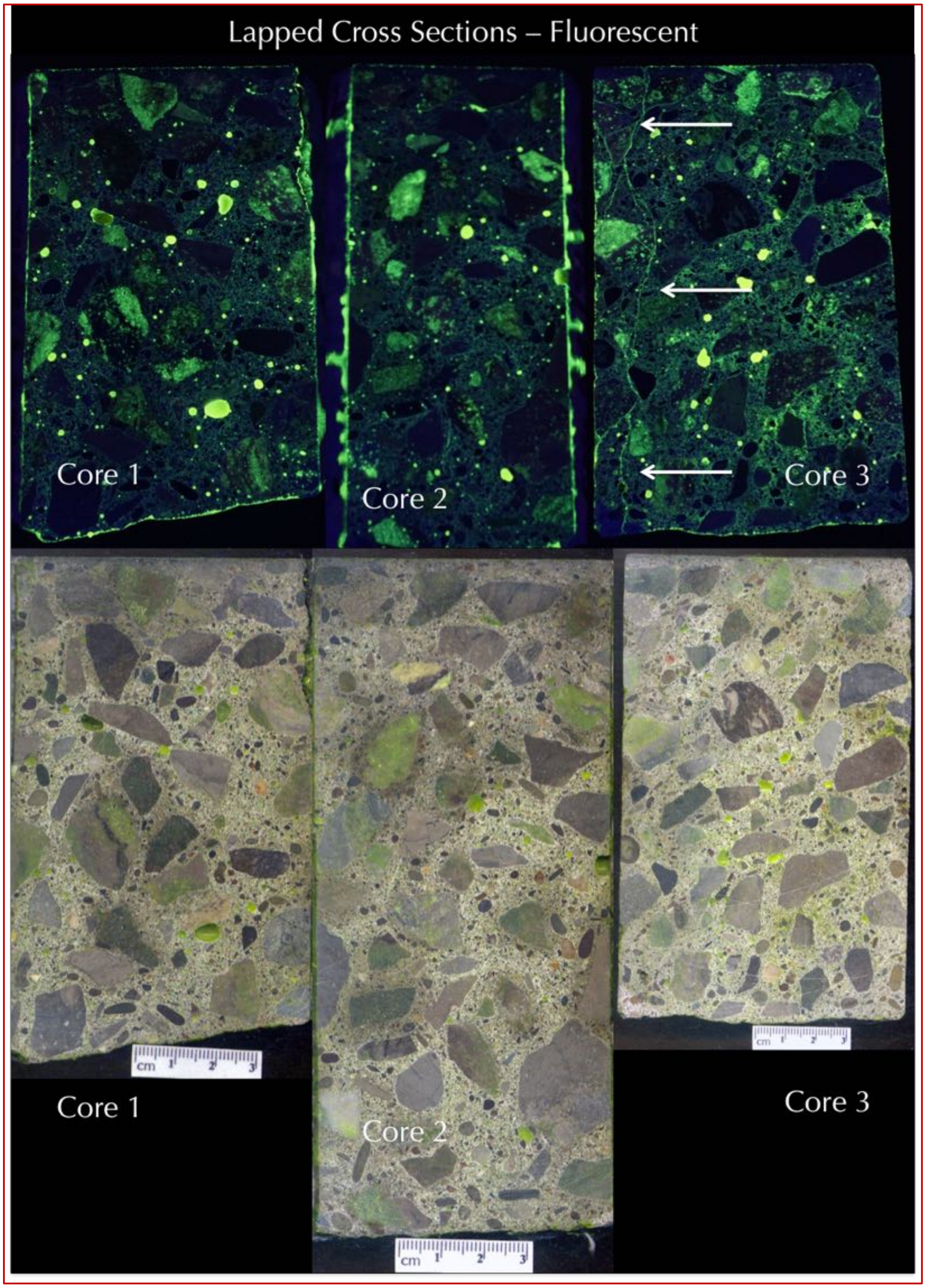

Figure 19: Observations of fluorescent dye-mixed epoxy-impregnated lapped cross sections (shown in the bottom row) in ultraviolet light (shown in top row) where cracks in the interior concrete are highlighted by fluorescent dye, mostly in Core 3 (arrows) as shown in the top row.

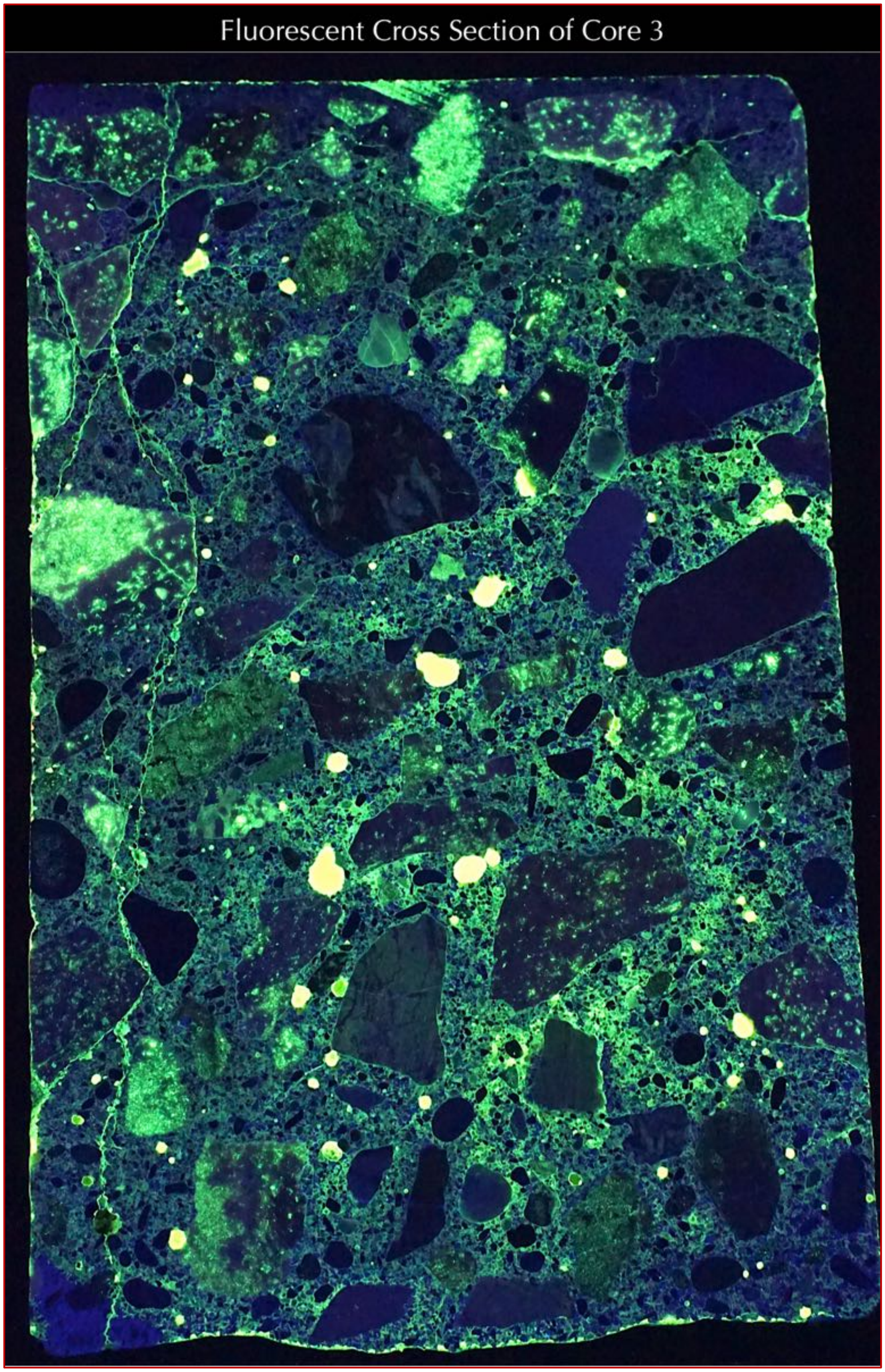

Figure 20: Observation of fluorescent dye-mixed epoxy-impregnated lapped cross section of Core 3 in ultraviolet light showing fine hairline microcracks at the surface region as well as through full depth of the core indicating extensive cracking of the concrete at this core location.

PHOTOMICROGRAPHS OF LAPPED CROSS SECTIONS

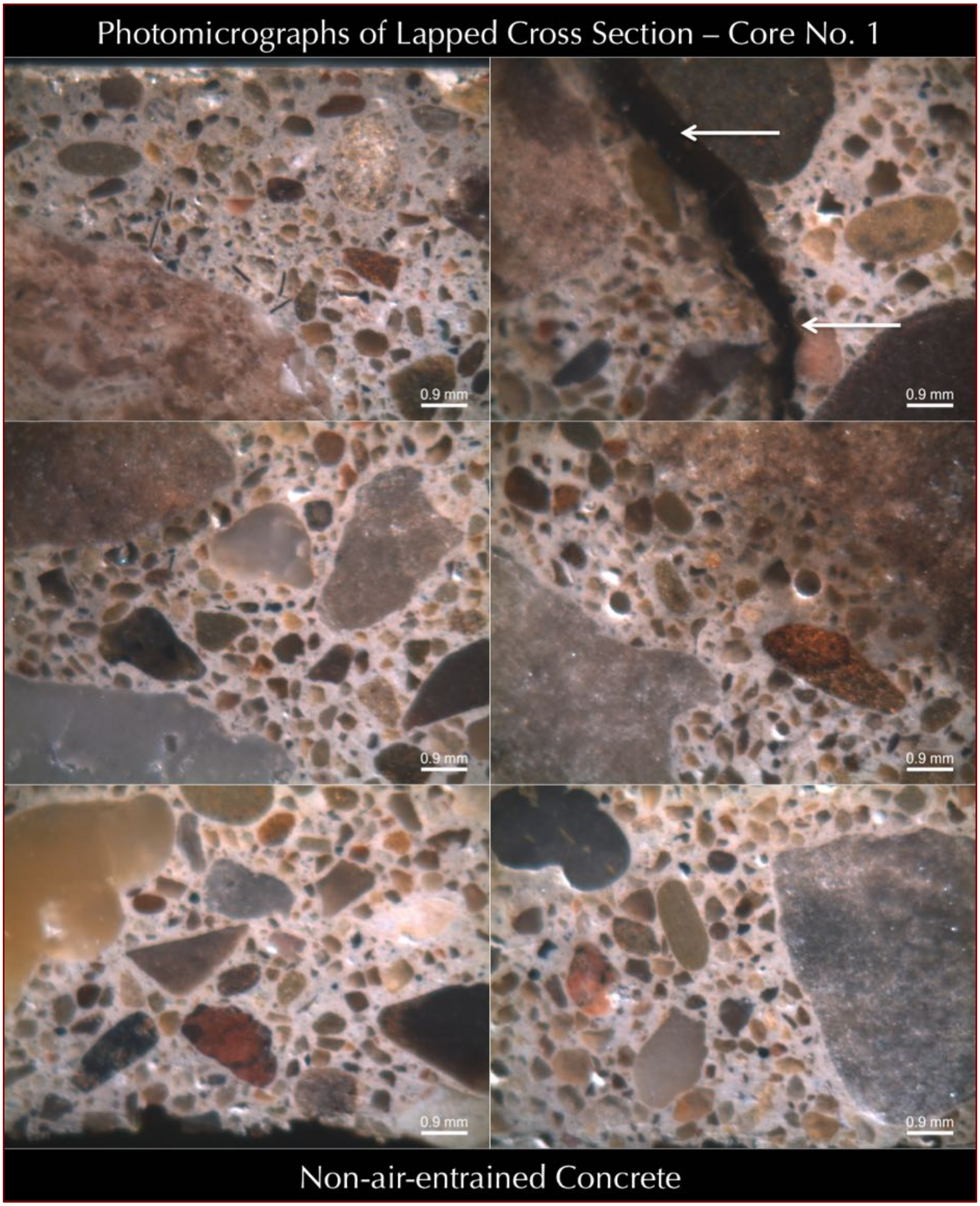

Figure 21: Photomicrographs of lapped cross section of Core 1 as seen in a low-power Stereozoom microscope showing: (a) overall non-air-entrained nature of concrete in all photos containing a few coarse near-spherical and irregularly-shaped entrapped air voids; (b) darker gray tone paste at the top trowel-finished surface region as opposed to relatively lighter toned paste in the interior body, and (c) major visible cracking in concrete (arrows).

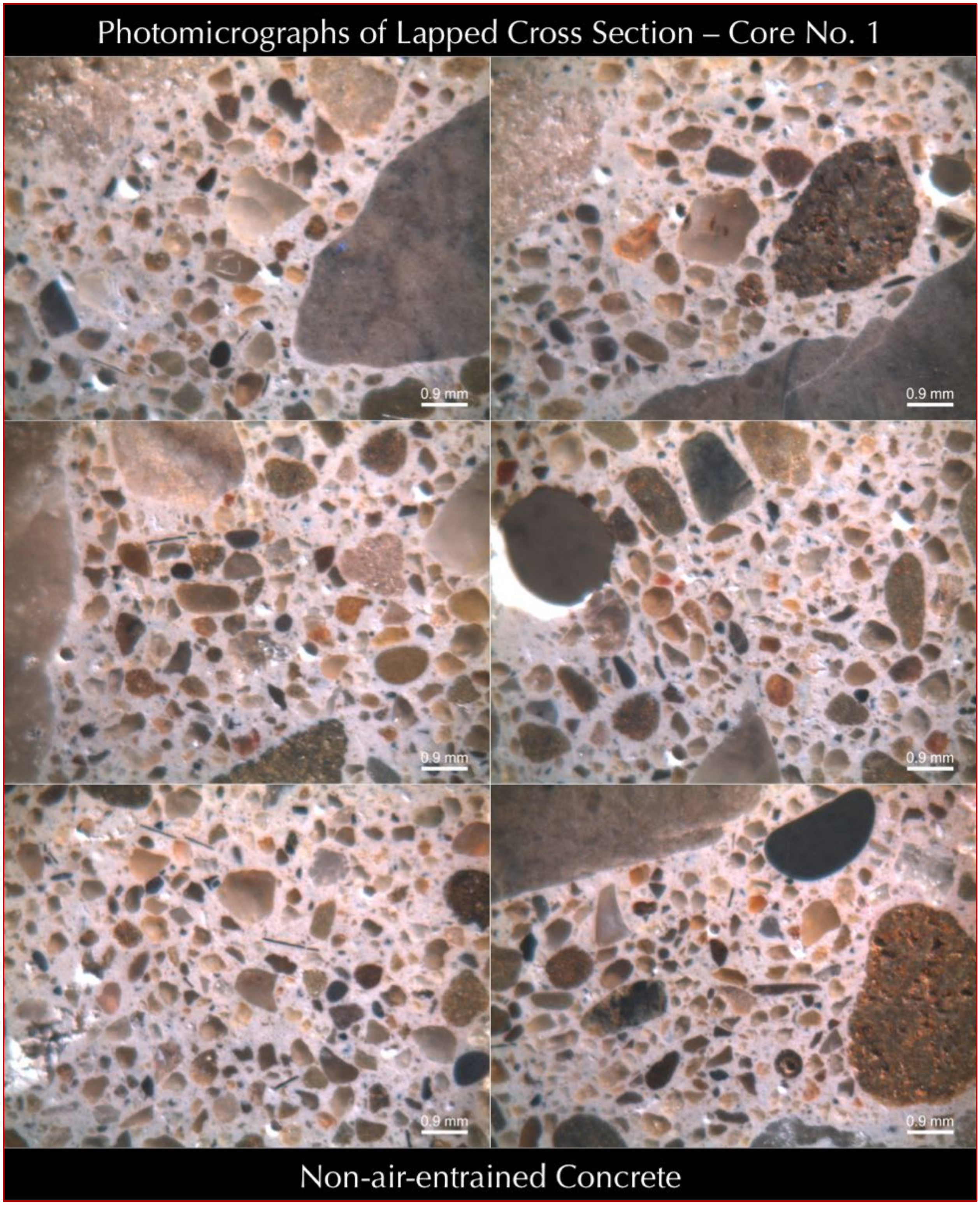

Figure 22: Photomicrographs of lapped cross section of Core 1 as seen in a low-power Stereozoom microscope showing overall non-air-entrained nature of concrete in all photos containing a few coarse near-spherical and irregularly-shaped entrapped air voids.

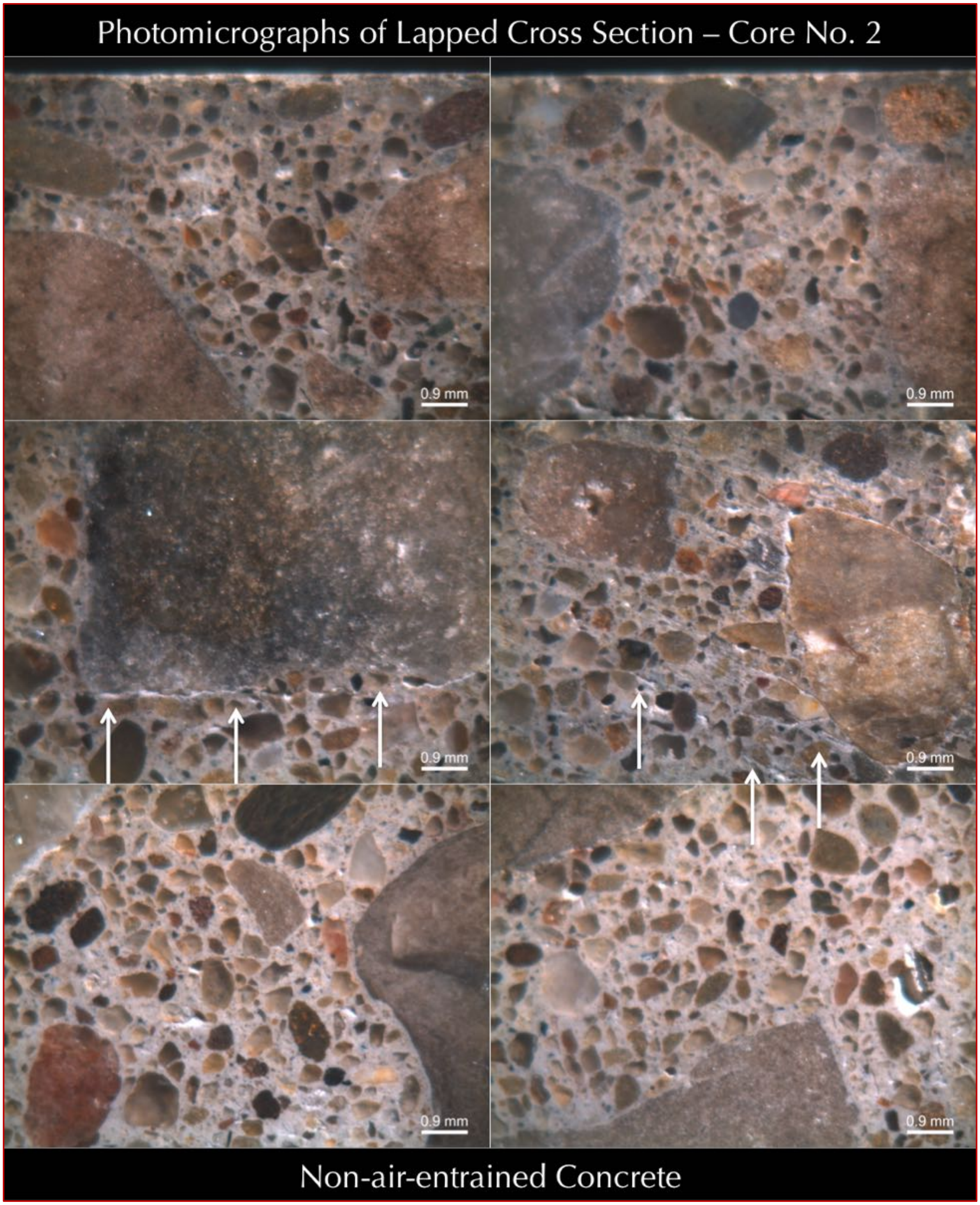

Figure 23: Photomicrographs of lapped cross section of Core 2 as seen in a low-power Stereozoom microscope showing: (a) overall non-air-entrained nature of concrete in all photos containing a few coarse near-spherical and irregularly-shaped entrapped air voids; (b) darker gray tone paste at the top trowel-finished surface region as opposed to relatively lighter toned paste in the interior body, and (c) some fine, hairline near-surface cracking at a depth of 10 to 15 mm from the finished surface (arrows in middle row) that are present despite no such cracking on the finished surface.

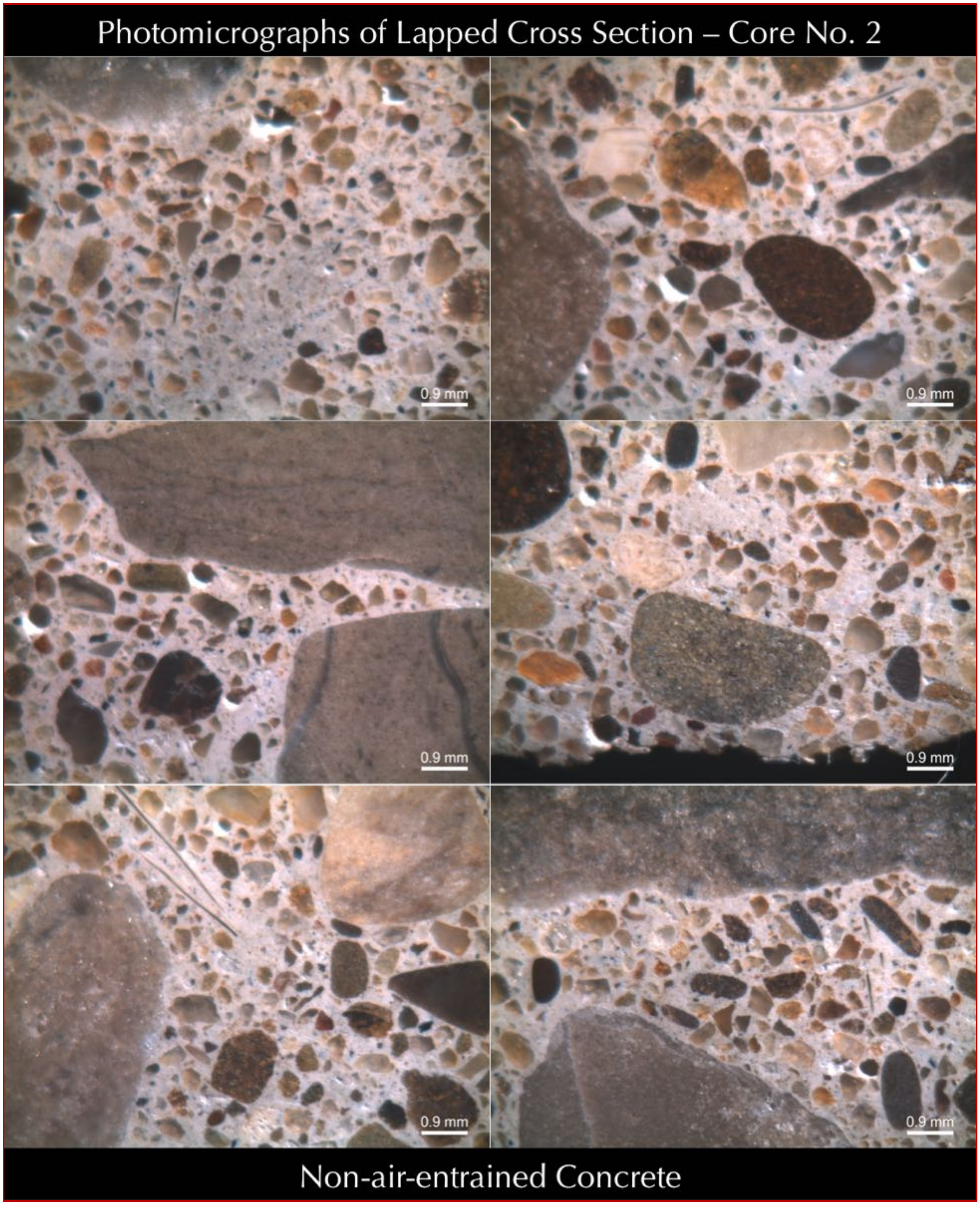

Figure 24: Photomicrographs of lapped cross section of Core 2 as seen in a low-power Stereozoom microscope showing overall non-air-entrained nature of concrete in all photos containing a few coarse near-spherical and irregularly-shaped entrapped air voids.

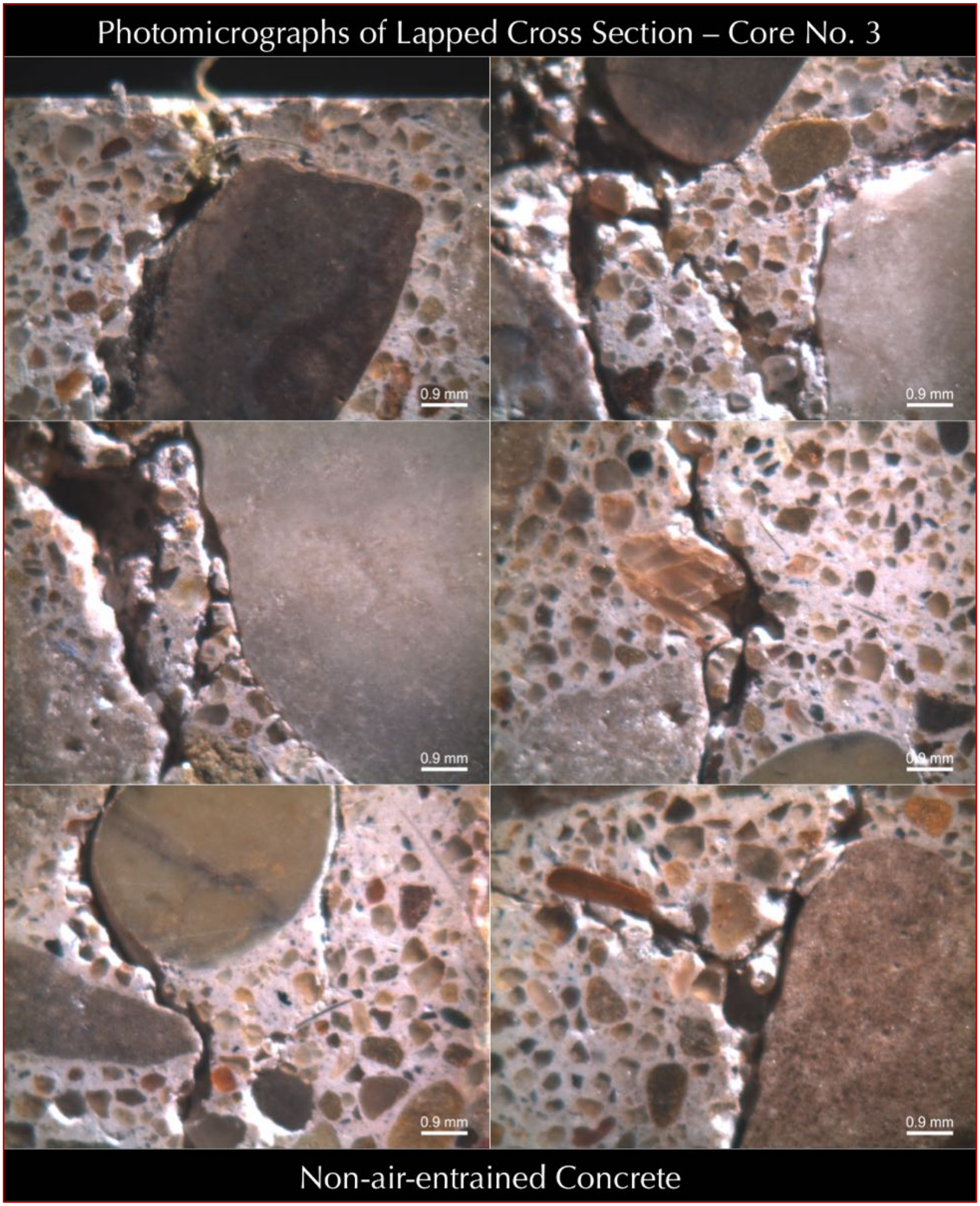

Figure 25: Photomicrographs of lapped cross section of Core 3 as seen in a low-power Stereozoom microscope showing: (a) overall non-air-entrained nature of concrete in all photos containing a few coarse near-spherical and irregularly-shaped entrapped air voids; (b) darker gray tone paste at the top trowel-finished surface region as opposed to relatively lighter toned paste in the interior body, and (c) extensive cracking in concrete. Notice some fine hairlike synthetic fibers sticking out of finished surface in the top left photo.

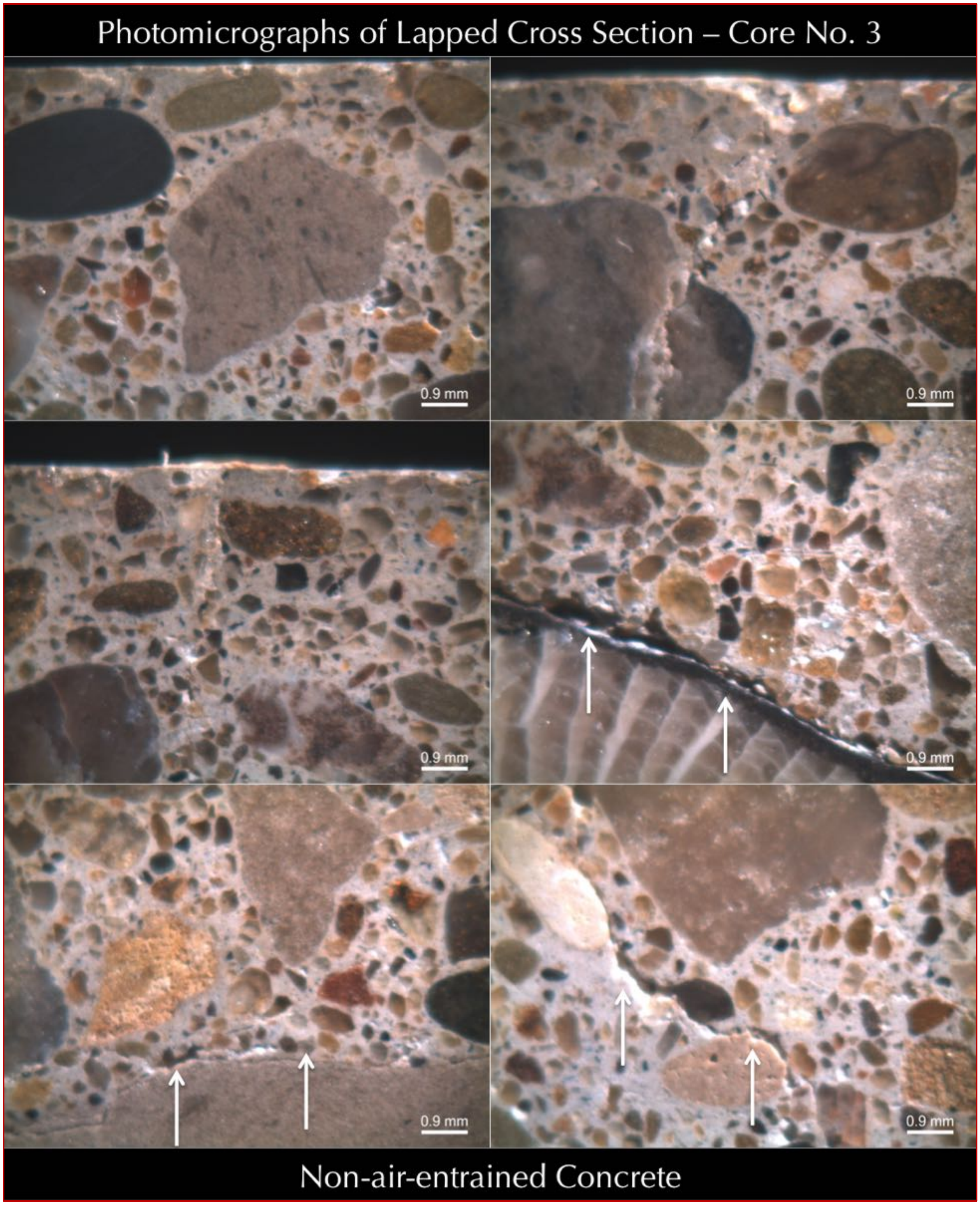

Figure 26: Photomicrographs of lapped cross section of Core 3 as seen in a low-power Stereozoom microscope showing: (a) overall non-air-entrained nature of concrete in all photos containing a few coarse near-spherical and irregularly-shaped entrapped air voids; (b) darker gray tone paste at the top trowel-finished surface region as opposed to relatively lighter toned paste in the interior body, and (c) extensive cracking in concrete. Notice some fine hairlike synthetic fibers sticking out of finished surface in middle left photo.

BLUE DYE-MIXED EPOXY-IMPREGNATED THIN SECTIONS

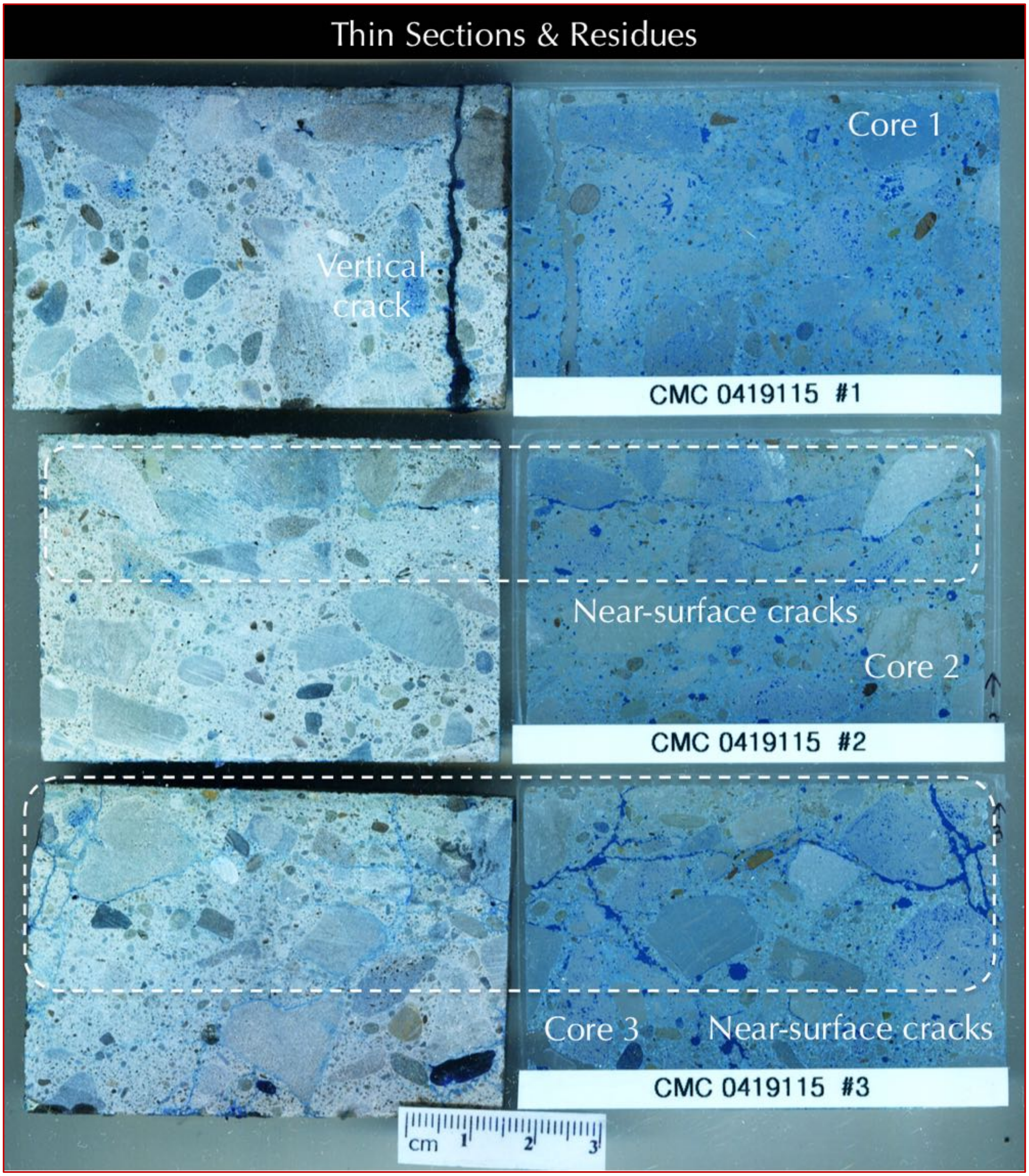

Figure 27: Blue dye-mixed epoxy-impregnated thin sections of cores from the top 2 inches highlighting cracks, voids, and porous regions of paste by the blue epoxy that has been absorbed more in those areas compared to denser regions. Boxed areas in Cores 2 and 3 show some cracks that are highlighted by the blue epoxy, especially in Core 2 at 10 to 15 mm depth from finished surface, which are also seen on the lapped cross section (Figures 16 and 23) as well as extensive cracking at the surface region of Core 3 within top 1 inch of finished surface (bottom row).

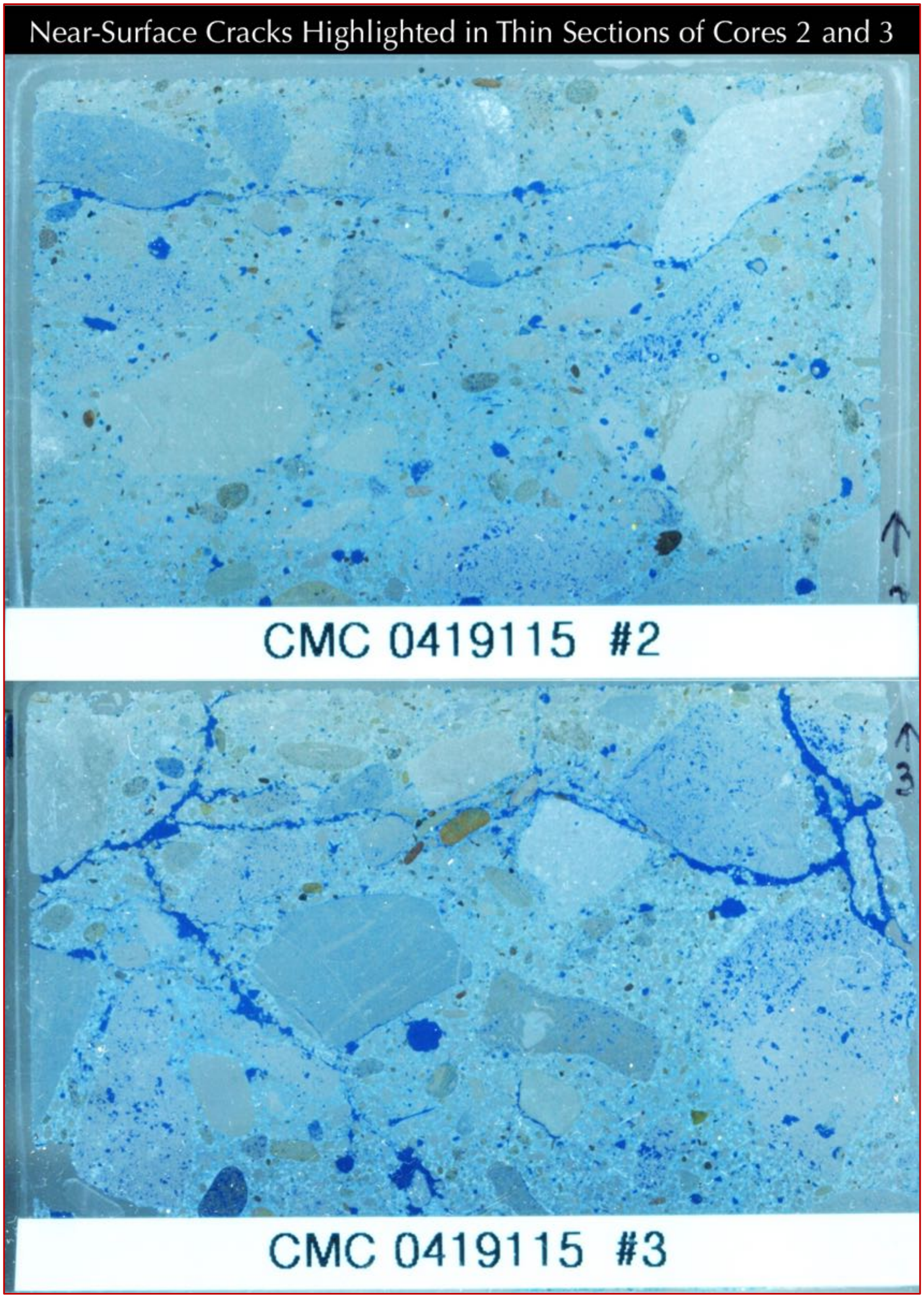

Figure 28: Enlarged views of thin sections of Cores 2 and 3 showing near-surface cracks that are highlighted by the blue epoxy, especially in Core 2 at 10 to 15 mm depth from finished surface (top), which are also seen on the lapped cross section (Figures 16 and 23) as well as extensive cracking at the surface region of Core 3 within top 1 inch of finished surface (bottom).

PHOTOMICROGRAPHS OF THIN SECTIONS

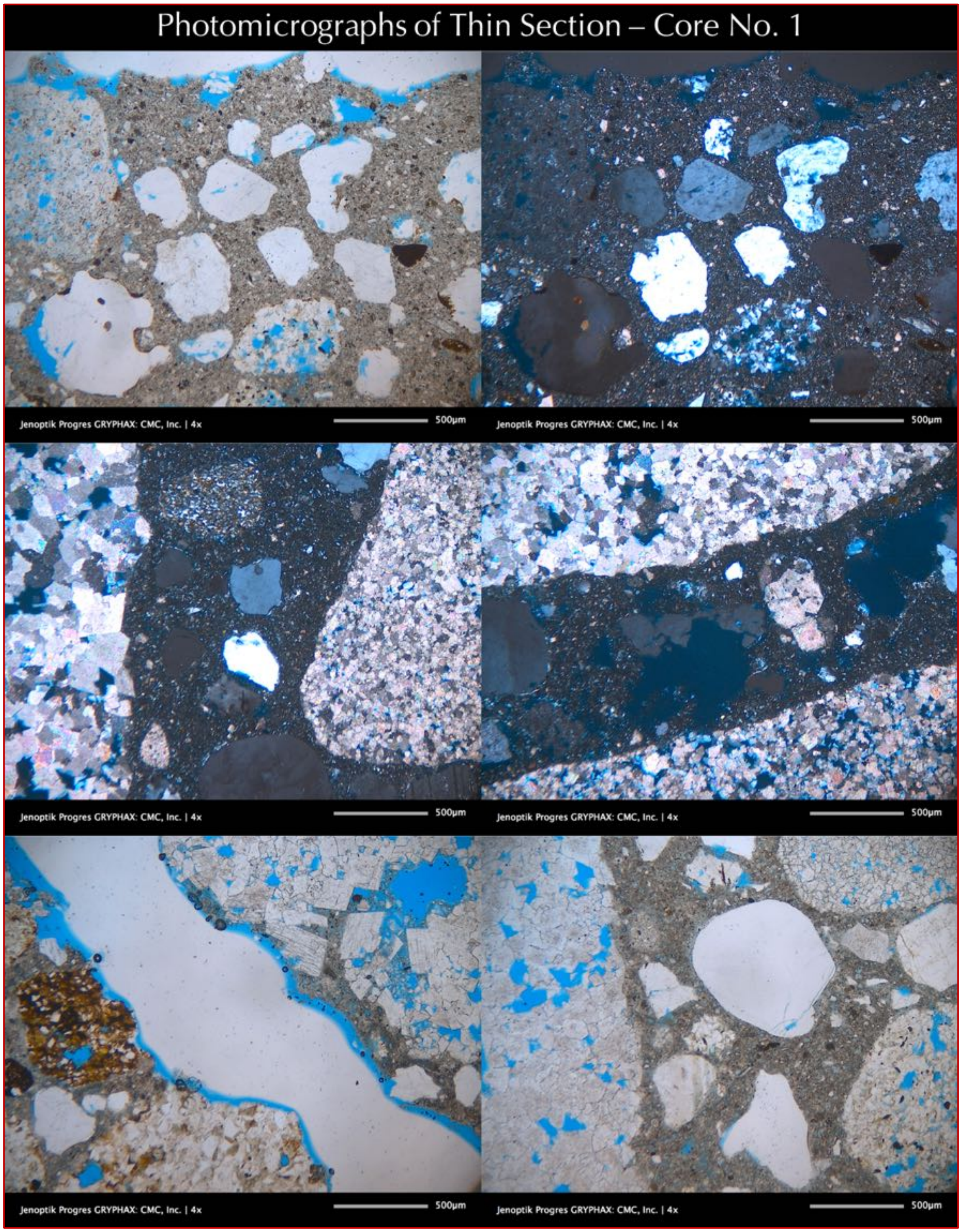

Figure 29: Photomicrographs of blue dye-mixed epoxy-impregnated thin section of concrete in Core 1 showing: (a) dense near-surface region of paste (top row) having abundant residual Portland cement and fine, angular, shard-like glassy ground granulated blast-furnace slag particles due to trowel-finishing operations; (b) crushed limestone-dolomite coarse aggregate and natural siliceous-calcareous sand fine aggregate (middle row); and (c) non-air-entrained concrete with visible cracking (bottom row).

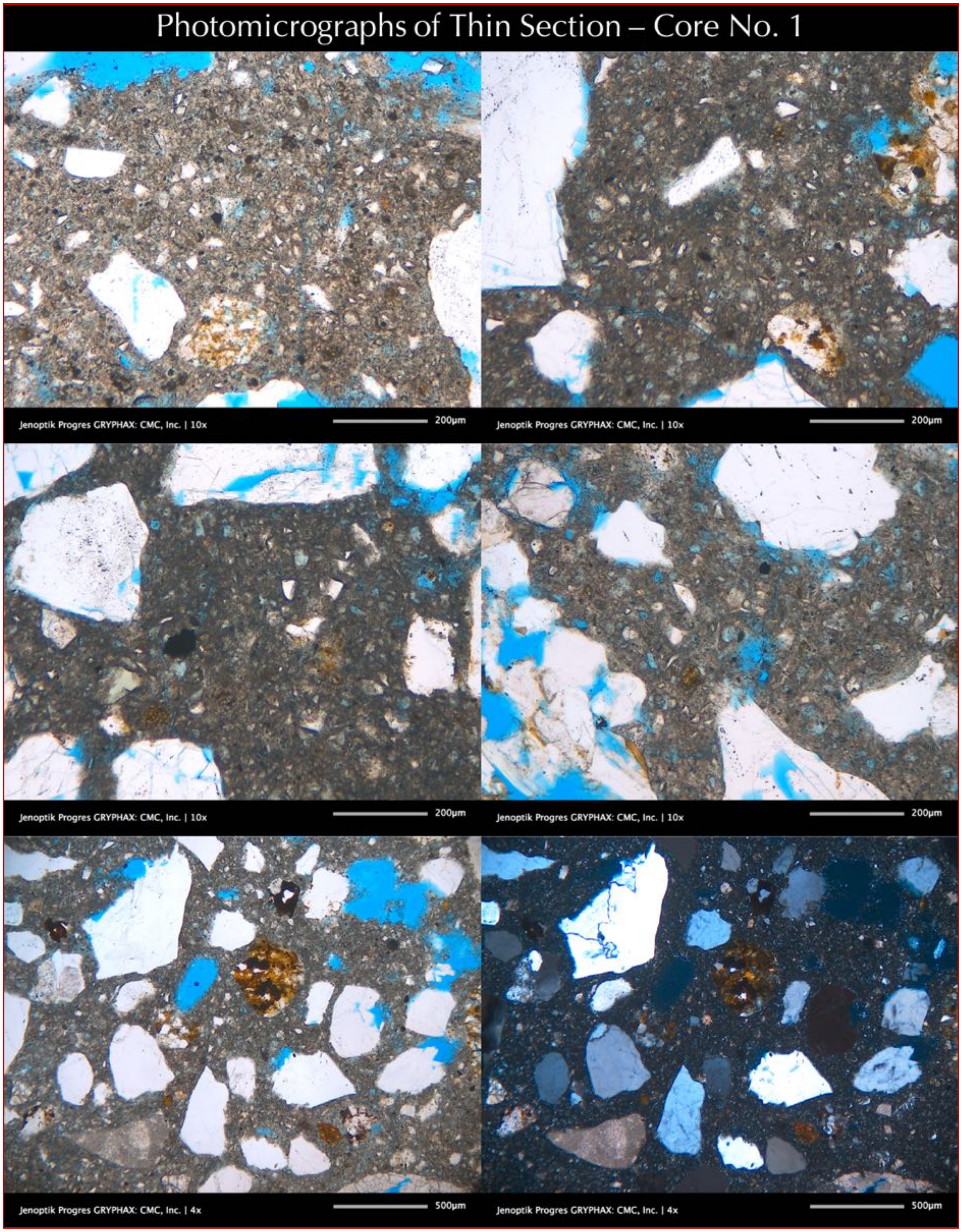

Figure 30: Photomicrographs of blue dye-mixed epoxy-impregnated thin section of concrete in Core 1 showing: (a) dense near-surface region of paste (top and middle rows) having abundant residual Portland cement and fine, angular, shard-like glassy ground granulated blast-furnace slag particles due to trowel-finishing operations; and (b) non-air-entrained non-carbonated interior concrete (bottom row).

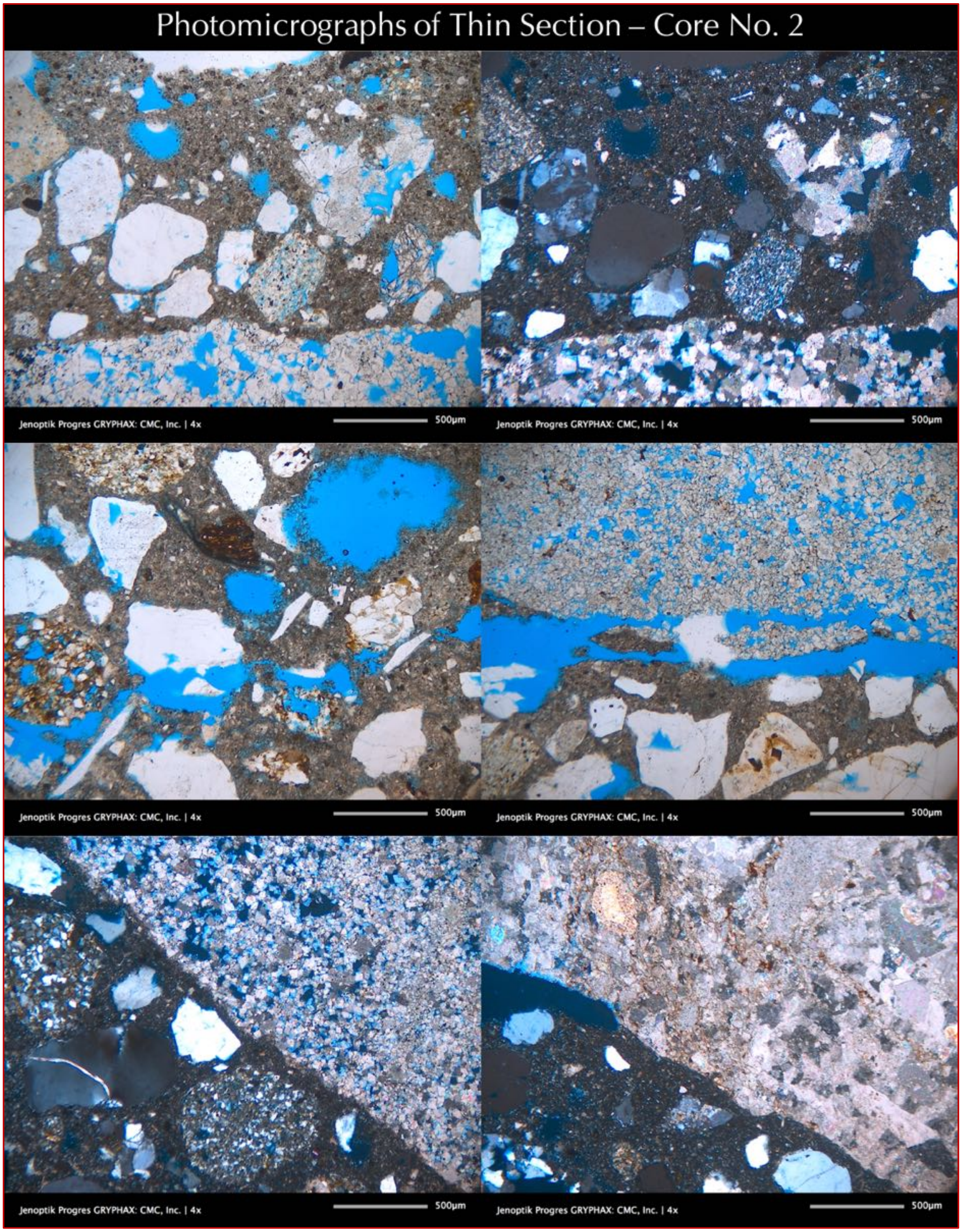

Figure 31: Photomicrographs of blue dye-mixed epoxy-impregnated thin section of concrete in Core 2 showing: (a) dense near-surface region of paste (top row) having abundant residual Portland cement and fine, angular, shard-like glassy ground granulated blast-furnace slag particles due to trowel-finishing operations; (b) crushed limestone-dolomite coarse aggregate and natural siliceous-calcareous sand fine aggregate (top and bottom rows); and (c) non-air-entrained concrete with near-surface cracking at a depth of 10 to 15 mm from surface (middle row).

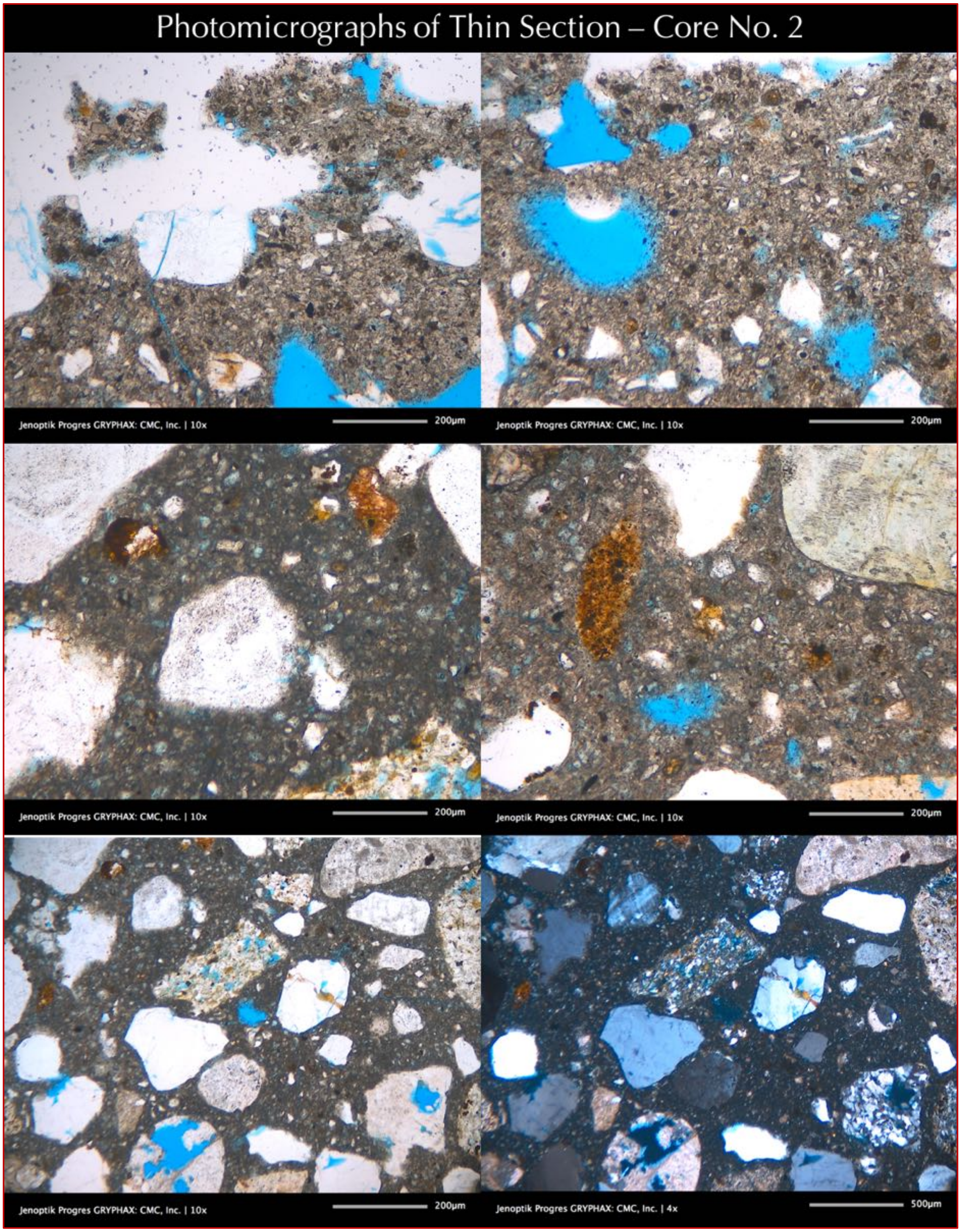

Figure 32: Photomicrographs of blue dye-mixed epoxy-impregnated thin section of concrete in Core 2 showing: (a) dense near-surface region of paste (top and middle rows) having abundant residual Portland cement and fine, angular, shard-like glassy ground granulated blast-furnace slag particles due to trowel-finishing operations; and (b) non-air-entrained non-carbonated interior concrete (bottom row).

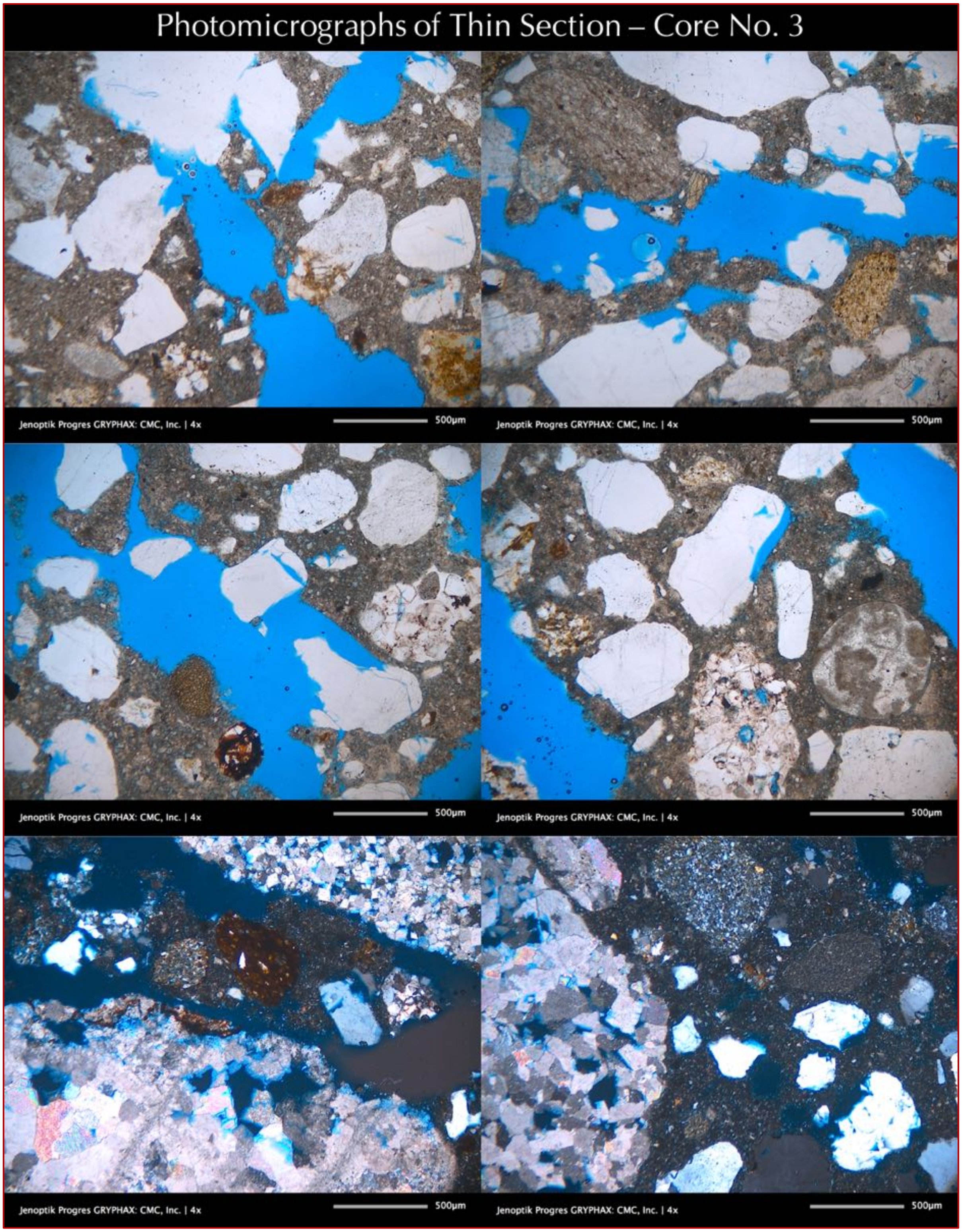

Figure 33: Photomicrographs of blue dye-mixed epoxy-impregnated thin section of concrete in Core 3 showing: (a) dense near-surface region of paste (top row) having abundant residual Portland cement and fine, angular, shard-like glassy ground granulated blast-furnace slag particles due to trowel-finishing operations and extensive cracking at the surface region; (b) crushed limestone-dolomite coarse aggregate and natural siliceous-calcareous sand fine aggregate (bottom row); and (c) non-air-entrained concrete with visible cracking (top and middle rows).

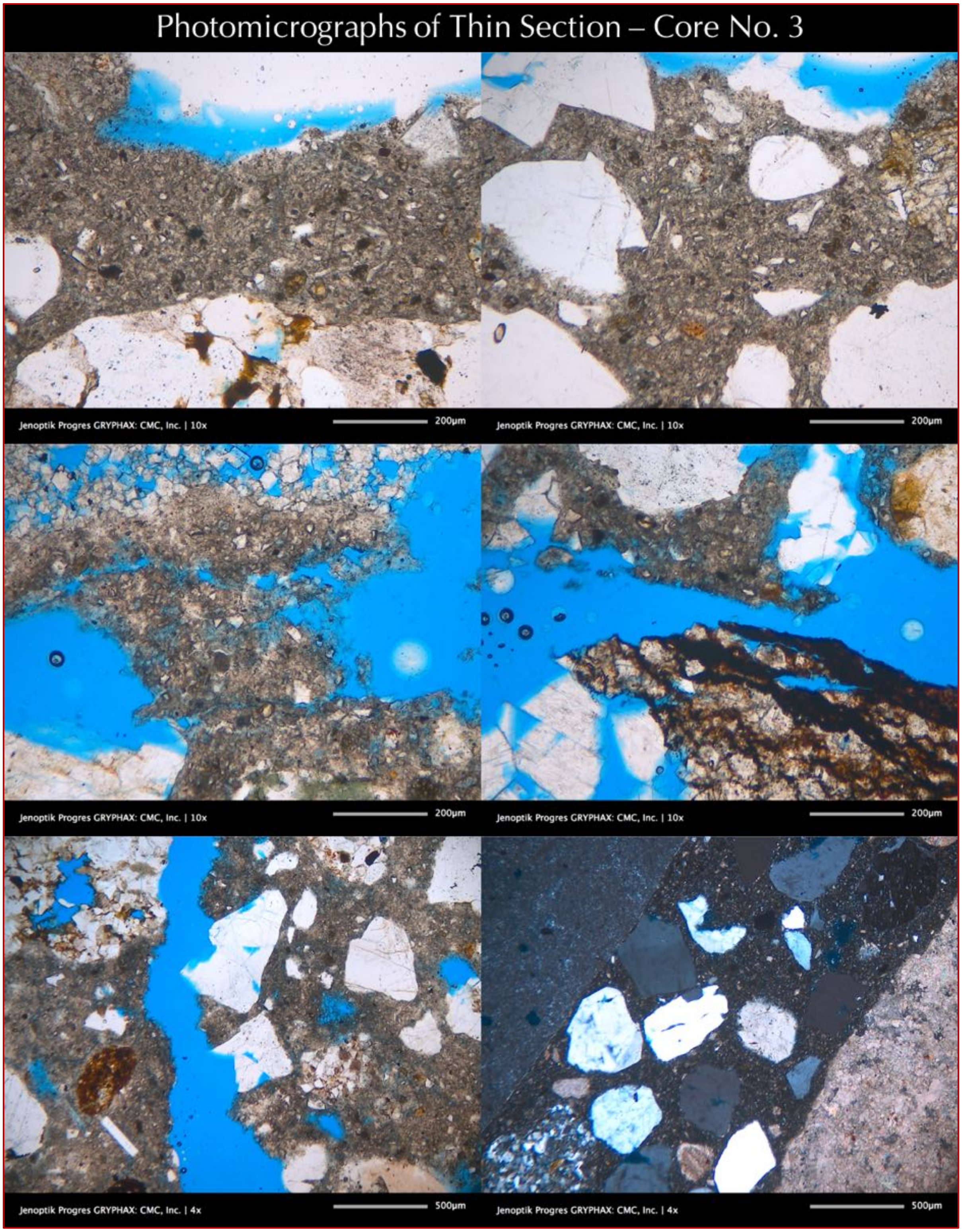

Figure 34: Photomicrographs of blue dye-mixed epoxy-impregnated thin section of concrete in Core 3 showing: (a) dense near-surface region of paste (top and middle rows) having abundant residual Portland cement and fine, angular, shard-like glassy ground granulated blast-furnace slag particles due to trowel-finishing operations; and (b) non-air-entrained non-carbonated interior concrete with extensive cracking (middle and bottom rows).

COARSE AGGREGATES

Coarse aggregates are compositionally similar in all three cores, which are crushed limestone-dolomite having nominal maximum sizes of 1 in. (25 mm) and containing major amounts of porous dolomite having variable intergranular porosities and subordinate amounts of limestone (biomicrite). Particles are medium to dark beige to tan colored, dense, hard, angular, massive textured, equidimensional to elongated, unaltered, uncoated, and uncracked.

Coarse aggregate particles are well-graded and well-distributed. There is no evidence of alkali-aggregate reactions of coarse aggregate particles in the cores. Coarse aggregate particles have been sound during their service in the concrete and did not contribute to the surface cracking of slab.

FINE AGGREGATES

Fine aggregates are compositionally similar natural siliceous-calcareous sands having major amounts of siliceous components (quartz, quartzite, feldspar, chert, siltstone, sandstone), subordinate amounts of calcareous components (limestone, dolomite), and minor amounts of argillaceous and ferruginous components (shale, ferruginous siltstone). Fine aggregates have nominal maximum sizes of $^{3}/_{8}$ in. (9.5 mm). Particles are variably colored, rounded to subangular, dense, hard, equidimensional to elongated, unaltered, uncoated, and uncracked.

Fine aggregate particles are well-graded and well-distributed. There is no evidence of alkali-aggregate reaction of fine aggregate particles. Fine aggregate particles have been sound during their service in the concrete.

The following Table summarizes properties of coarse and fine aggregates in all three cores.

Properties and Compositions of Aggregates	Core No. 1	Core No. 2	Core No. 3
Coarse Aggregate			
Types	Crushed Dolomite - Limestone		
Nominal maximum size (in.)	1 in. (25 mm)		
Rock Types	Porous dolomite having variable intergranular porosities and subordinate amounts of limestone (biomicrite)		
Angularity, Density, Hardness, Color, Texture, Sphericity	Angular, dense, hard, dark gray, massive textured, equidimensional to elongated		
Cracking, Alteration, Coating	Unaltered, Uncoated, and Uncracked		
Grading & Distribution	Well-graded and Well-distributed		
Soundness	Sound		
Alkali-Aggregate Reactivity	None		

Properties and Compositions of Aggregates	Core No. 1	Core No. 2	Core No. 3
Fine Aggregate			
Types	Natural siliceous-calcareous sand		
Nominal maximum size (in.)	$^3/_8$ in. (9.5 mm)		
Rock Types	Major amounts of siliceous components (quartz, quartzite, feldspar, chert, siltstone), subordinate amounts of calcareous components (limestone, dolomite), and minor amount of argillaceous and ferruginous components (shale, ferruginous siltstone)		
Cracking, Alteration, Coating	Variably colored, rounded to subangular, dense, hard, equidimensional to elongated		
Grading & Distribution	Well-graded and Well-distributed		
Soundness	Sound		
Alkali-Aggregate Reactivity	None		

Table 1: Properties of coarse and fine aggregates of concrete.

PASTE

Properties and composition of hardened cement paste are summarized in Table 2. Paste in all three cores are compositionally similar, medium gray, denser and darker gray at the top 5 to 6 mm due to trowel finishing operations. Paste in the interior bodies of cores are dense and hard; freshly fractured surfaces of interior paste have subvitreous lusters and subconchoidal textures. Residual and relict Portland cement particles are present and estimated to constitute 6 to 8 percent of the paste volumes. Distributed throughout the paste are fine, angular, shard-like glassy particles of ground granulated blast furnace slag having the fineness of Portland cement. Hydration of Portland cement is normal.

Properties and Compositions of Paste	Core No. 1	Core No. 2	Core No. 3
Color, Hardness, Porosity, Luster	Medium gray, denser and darker gray at the top 5 to 6 mm due to trowel finishing operations. Paste in the interior bodies of cores are dense and hard; freshly fractured surfaces of interior paste have subvitreous lusters and subconchoidal textures		
Residual Portland Cement Particles	Normal, 6 to 8 percent by paste volume		
Calcium hydroxide from cement hydration	Normal, 10 to 14 percent by paste volume		
Pozzolans, Slag, etc.	Distributed throughout the paste are fine, angular, shard-like glassy particles of ground granulated blast furnace slag having the fineness of Portland cement		
Water-cementitious materials ratio (*w/cm*), estimated	0.40 to 0.44 in the body but less than 0.40 at the finished surface region		
Cement Content (bags per cubic yard)	7 to $7^1/_2$ of which 25 to 30 percent is estimated to be ground granulated blast furnace slag		
Secondary Deposits	None		
Depth of Carbonation, mm	1 to 2 mm at the finished surface region		

Properties and Compositions of Paste	Core No. 1	Core No. 2	Core No. 3
Microcracking	Craze cracking and other near-surface fine microcracking from shrinkage and possible early freezing of concrete		
Aggregate-paste Bond	Tight		
Bleeding, Tempering	None		
Chemical deterioration	None		

Table 2: Proportions and composition of hardened cement paste.

The textural and compositional features of the paste are indicative of cementitious materials contents similar in all three cores and estimated to be equivalent to 7 to 7½ bags of Portland cement per cubic yard of which 25 to 30 percent is estimated to be ground granulated blast furnace slag, and, water-cementitious materials ratio (*w/cm*) estimated to be 0.40 to 0.44 in the body but less than 0.40 at the finished surface region.

There is no evidence of any deleterious deposits found in the cores. Carbonation is shallow 1 to 2 mm. Bonds between the coarse and fine aggregate particles and paste are tight. There is no evidence of microcracking due to any chemical deteriorations, except for some craze cracking and other near-surface fine microcracking from shrinkage and possible early freezing of concrete.

The overall quality and condition of the concrete in the interior bodies of the cores i.e. beneath the finished surface and away from visible cracks are judged to be dense, well-consolidated with no evidence of any physical or chemical deterioration.

However, due to the observed non-air-entrained nature of the concrete in all cores, along with very dense nature of paste, estimated low *w/cm*, high cementitious materials content, all of which are consistent with very high 28-day compressive strengths of cylinders (170 percent higher than the design strength) drying shrinkage and possible early freezing of concrete without a heated enclosure are judged to have played roles in causing the visible cracks on the surface and underneath.

AIR

Air occurs as a few coarse, near-spherical and irregularly shaped voids of sizes coarser than 1 mm that are characteristic of entrapped air. Air-void systems of concrete in all three cores are suggestive of no intentional addition of an air-entraining agent in the mix.

Concretes in all cores are found to be non-air-entrained, having air contents estimated from petrographic examinations to be 1 to 2 percent.

CHEMICAL PROFILES

POTENTIOMETRIC TITRATION (WATER-SOLUBLE CHLORIDE)

Water-soluble chloride contents were determined at the top finished surface region (within the top 0.5 in.), at mid-depth location, and bottom end of the cores, as shown in Figures 35 and 37. Table 3 summarizes results of water-soluble chloride contents, where first column shows the sample identification, second column shows the depth from where sections for chloride analyses were taken, third column shows the raw chloride content data as percent chloride in the concrete by mass of the sample, forth column represents percent chloride content in the sample by mass of cement by assuming 15 percent Portland cement content in the concrete and normal-weight concrete (i.e. by dividing the raw chloride contents by mass of 'concrete' by 0.15 to obtain chloride contents by mass of 'cement'), fifth column converts the raw chloride content in concrete from weight percent to ppm by multiplying the third column data by 10,000, and the last column is only applicable if the chloride found in concrete is obtained not from the external environment but from the use of flake (anhydrous) calcium chloride as a set-accelerating admixture in solution, in which case the data in the last column represents equivalent flake calcium chloride added to the mix as an accelerating admixture. This last column data can be discarded if there is no evidence of addition of a chloride-containing set-accelerating admixture in the concrete, as appeared to be the case here.

Sample ID	Location	Percent Water Soluble Chloride by Mass of Sample	Percent Acid Soluble Chloride by Mass of Cement[1] (% Chloride by Mass of Sample/0.15)	Percent Acid Soluble Chloride PPM (% Chloride by Mass of Sample x 10000)	Equivalent Flake Calcium Chloride (% Chloride by Mass of Cement x 2.07)
Core No. 1	Top	0.0071	0.047	71	0.01
	Mid-Depth	0.0065	0.043	65	0.01
	Bottom	0.0061	0.041	61	0.01
Core No. 2	Top	0.0111	0.074	111	0.02
	Mid-Depth	0.0080	0.053	80	0.02
	Bottom	0.0145	0.097	145	0.03
Core No. 3	Top	0.0141	0.094	141	0.03
	Mid-Depth	0.0120	0.080	120	0.02
	Bottom	0.0062	0.041	62	0.01

Table 3: Water-soluble chloride contents from the top, mid-depth, and bottom locations of cores. [1]Assuming a cementitious materials content of 15 percent by mass of a normal-weight concrete.

ION CHROMATOGRAPHY (WATER-SOLUBLE ANIONS AND CATIONS)

Water-soluble anions and cations from the top, mid-depth, and bottom ends of cores are shown in Figures 38, 39, and 40 and in the following Table 4.

Results show no preferential enrichments of chlorides, sulfates, alkalis, and calcium at the finished surface regions compared to the interiors, which are indicative of no moisture migration through the slab towards the top to create a chemical profile or exposure to any chloride-containing admixture or deicers.

Sample ID	Location	Percent by weight of concrete of water-soluble anions from Ion Chromatography			Percent by weight of concrete of water-soluble anions from Ion Chromatography		
		Chloride	Nitrate	Sulfate	Sodium	Potassium	Calcium
Core No. 1	Top	0.006	0.036	0.002	0.011	0.024	0.334
	Middle	0.005	0.031	0.003	0.015	0.035	0.373
	Bottom	0.005	0.041	0.005	0.014	0.036	0.378
Core No. 2	Top	0.010	0.046	0.002	0.018	0.043	0.398
	Middle	0.006	0.037	0.001	0.018	0.043	0.382
	Bottom	0.006	0.043	0.002	0.013	0.026	0.397
Core No. 3	Top	0.006	0.065	0.001	0.013	0.026	0.339
	Middle	0.004	0.067	0.001	0.017	0.046	0.342
	Bottom	0.005	0.064	0.001	0.016	0.042	0.382

Table 4: Water-soluble anions and cations from the top, mid-depth, and bottom locations of cores determined from ion chromatography.

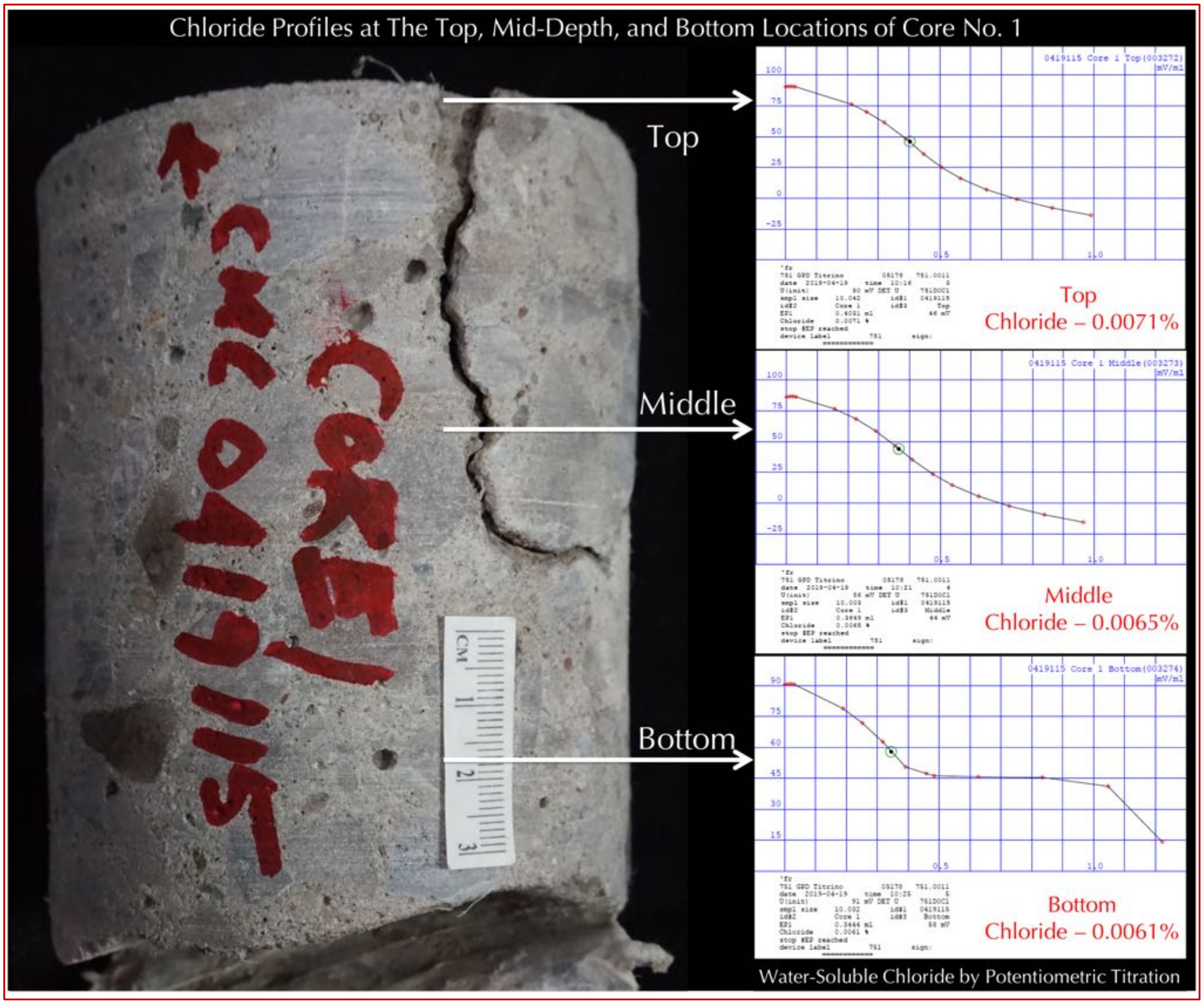

Figure 35: The potentiometric titration curves of chloride analyses from the top (top right), mid-depth location (middle right), and bottom end (bottom right) of Core No. 1 (left column). In all titration curves, the equivalent point of titration is marked with a dot and circle. Chloride content is shown both in the data from the Metrohm Titrator as well as in red. Notice negligible chloride contents at all depths indicating absence of any chloride-containing set accelerating chemicals in the concrete mix, or any deicing chemicals at the surface during service.

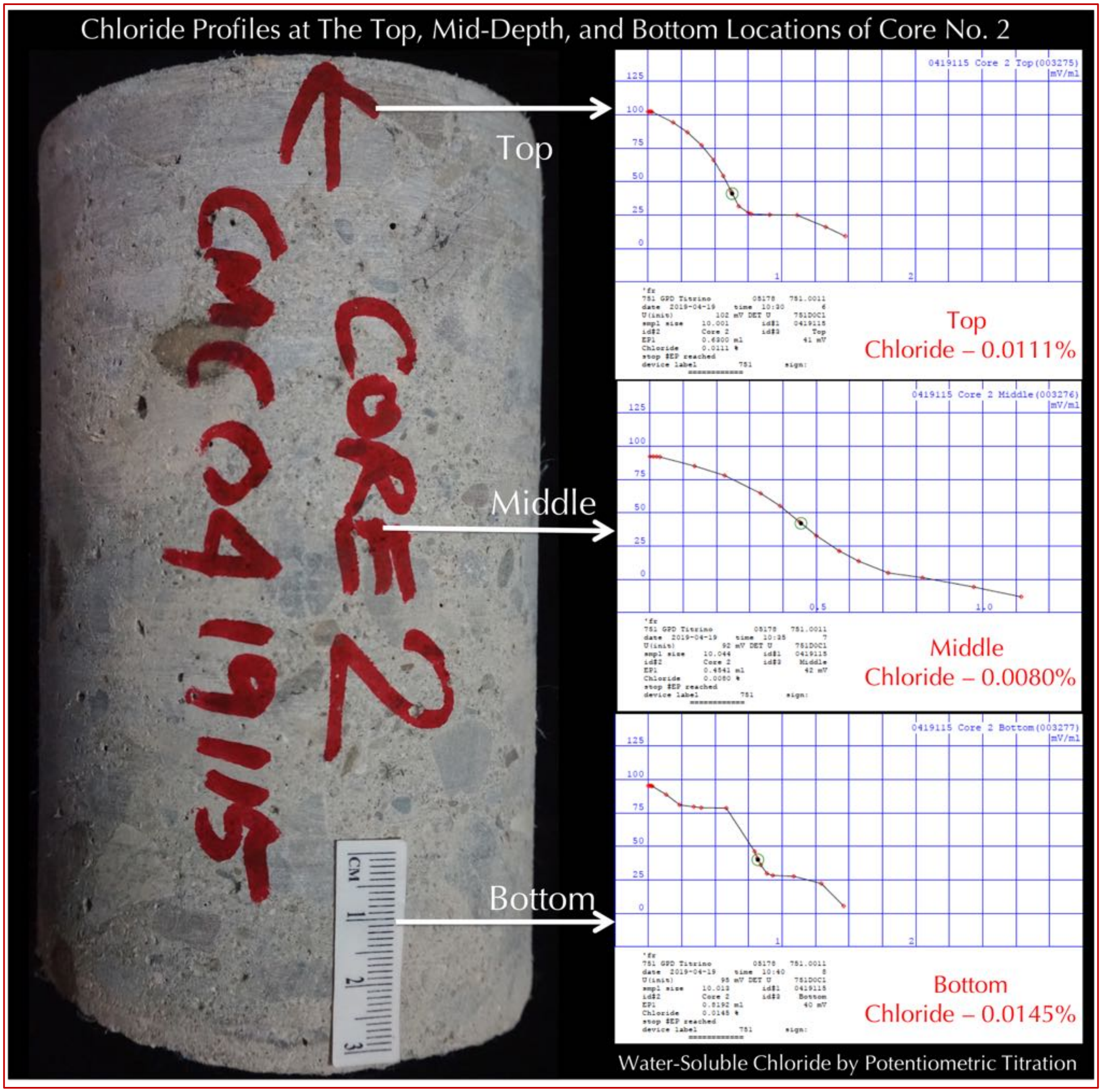

Figure 36: The potentiometric titration curves of chloride analyses from the top (top right), mid-depth location (middle right), and bottom end (bottom right) of Core No. 2 (left column). In all titration curves, the equivalent point of titration is marked with a dot and circle. Chloride content is shown both in the data from the Metrohm Titrator as well as in red. Notice negligible chloride contents at all depths indicating absence of any chloride-containing set accelerating chemicals in the concrete mix, or any deicing chemicals at the surface during service.

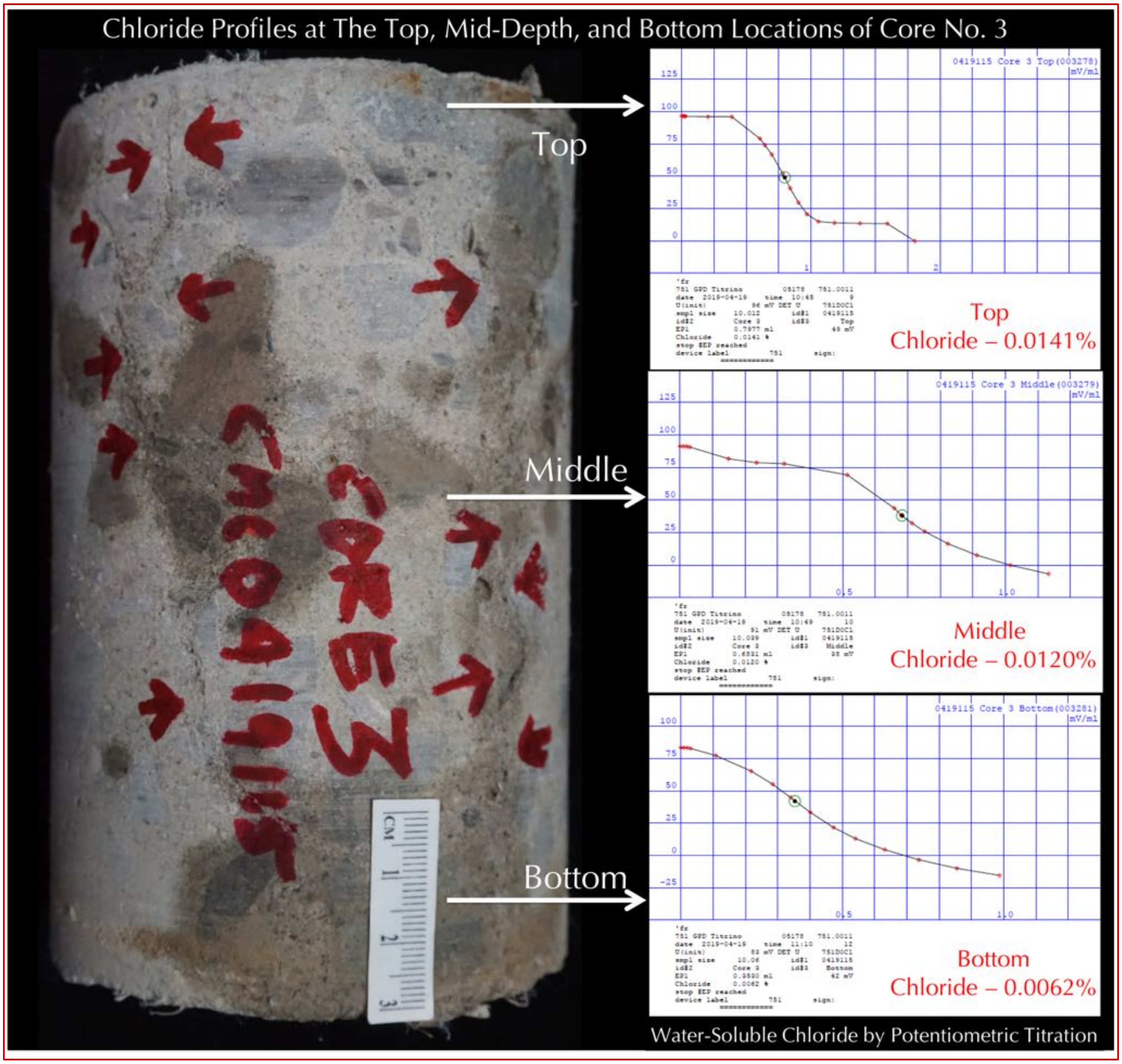

Figure 37: The potentiometric titration curves of chloride analyses from the top (top right), mid-depth location (middle right), and bottom end (bottom right) of Core No. 3 (left column). In all titration curves, the equivalent point of titration is marked with a dot and circle. Chloride content is shown both in the data from the Metrohm Titrator as well as in red. Notice negligible chloride contents at all depths indicating absence of any chloride-containing set accelerating chemicals in the concrete mix, or any deicing chemicals at the surface during service.

Chemical Profiles at The Top, Mid-Depth, and Bottom Locations of Core No. 1

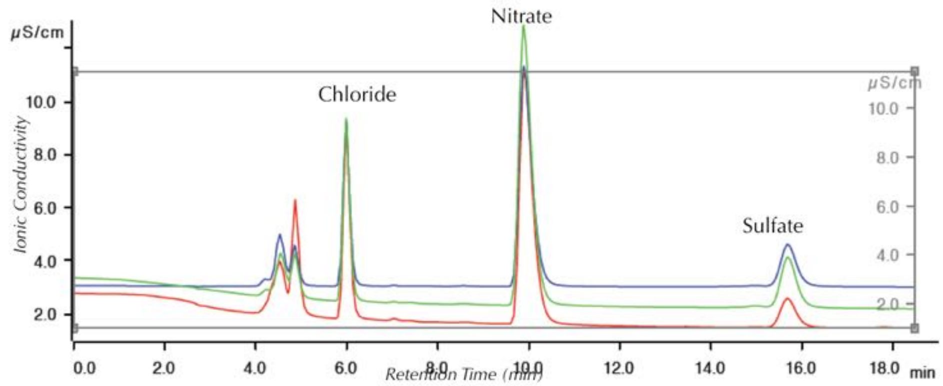

	Ident	... ...	Method	Analysis	Legend	Display
1	S1-CMC 0419115 Core 1 Top	... 1 ... ... 1. 1.	MiVDT 4.0_Anion_UF_i-dilution by area_No D	Anions		on
2	S2-CMC 0419115 Core 1 Middle	... 2 ... ... 1. 1.	MiVDT 4.0_Anion_UF_i-dilution by area_No D	Anions		on
3	S3-CMC 0419115 Core 1 Bottom	... 3 ... ... 1. 1.	MiVDT 4.0_Anion_UF_i-dilution by area_No D	Anions		on

Metrohm 881 Professional IC and 858 Sample Processor, in-vial dilution method, Sodium carbonate-bicarbonate eluent

Depth	Chloride (%)	Nitrate (%)	Sulfate (%)
Top	0.006	0.036	0.002
Middle	0.005	0.031	0.003
Bottom	0.005	0.041	0.005

Anion % Weight in the Table = [(In-vial concentration from IC including Dilution Factor shown by curves, ppm) × (Original Filtrate Volume, mL)] ÷ [(Sample Weight, g) × (10,000 for ppm to wt.% conversion)]

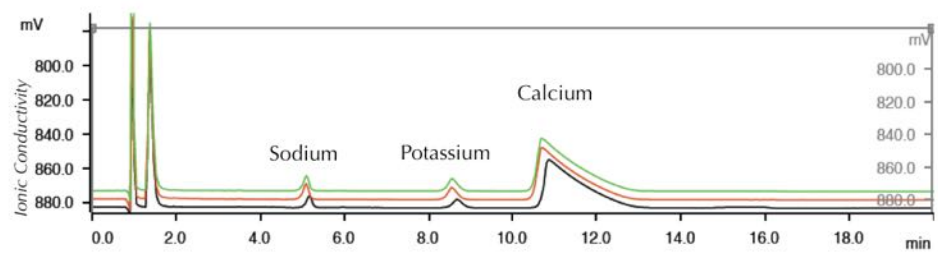

	...	...	Ident	...	...	S...		Method	...	Legend	Display
1	...	1	S1 - CMC 0419115 Core 1 Top	...	...	1.0	1.0	CMC Cations	...		on
2	...	2	S2 - CMC 0419115 Core 1 Middle	...	...	1.0	1.0	CMC Cations	...		on
3	...	3	S3 - CMC 0419115 Core 1 Bottom	...	...	1.0	1.0	CMC Cations	...		on

Metrohm 861 Advanced Compact IC and 788 Sample Processor, Nitric/Dipicolinic Acid eluent

Depth	Na (wt.%)	K (wt.%)	Ca (wt.%)
Top	0.011	0.024	0.334
Middle	0.015	0.035	0.373
Bottom	0.014	0.036	0.378

Cation % Weight in the Table = [(In-vial concentration from IC including Dilution Factor shown by curves, ppm) × (Original Filtrate Volume, mL)] ÷ [(Sample Weight, g) × (10,000 for ppm to wt.% conversion)]

Figure 38: Results of ion chromatography of water-soluble anions (chloride, nitrate, sulfate) at the top, and, water-soluble cations (sodium, potassium, and calcium) at the bottom of deionized water-digested pulverized concrete from the top, mid-depth, and bottom locations of Core No. 1 showing no sign of preferential enrichment of chloride, sulfate, alkalis, and calcium at the surface region compared to interior i.e. beyond the amounts detected that are judged to be from the concrete-making ingredients. Tables beneath ion chromatograms show results as percent by mass of concrete for anions and cations.

Chemical Profiles at The Top, Mid-Depth, and Bottom Locations of Core No. 2

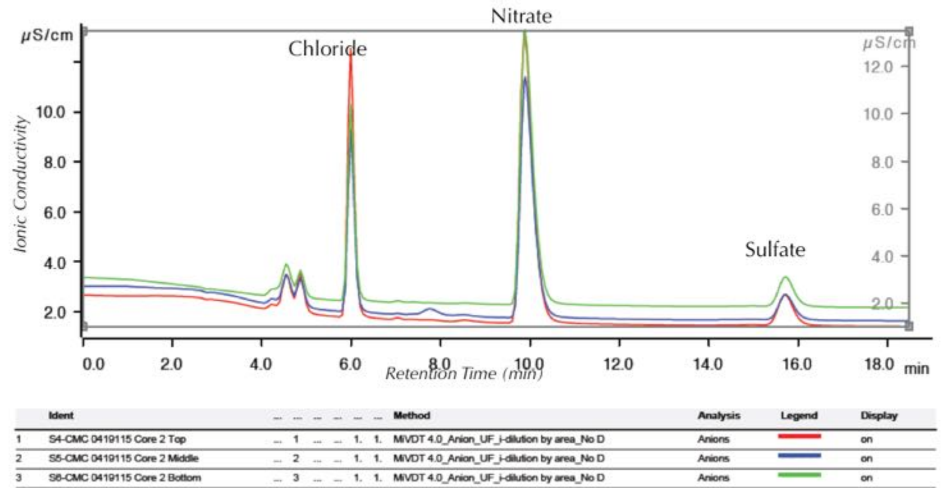

Metrohm 881 Professional IC and 858 Sample Processor, in-vial dilution method, Sodium carbonate-bicarbonate eluent

Depth	Chloride (%)	Nitrate (%)	Sulfate (%)
Top	0.010	0.046	0.002
Middle	0.006	0.037	0.001
Bottom	0.006	0.043	0.002

Anion % Weight in the Table = [(In-vial concentration from IC including Dilution Factor shown by curves, ppm) × (Original Filtrate Volume, mL)] ÷ [(Sample Weight, g) × (10,000 for ppm to wt.% conversion)]

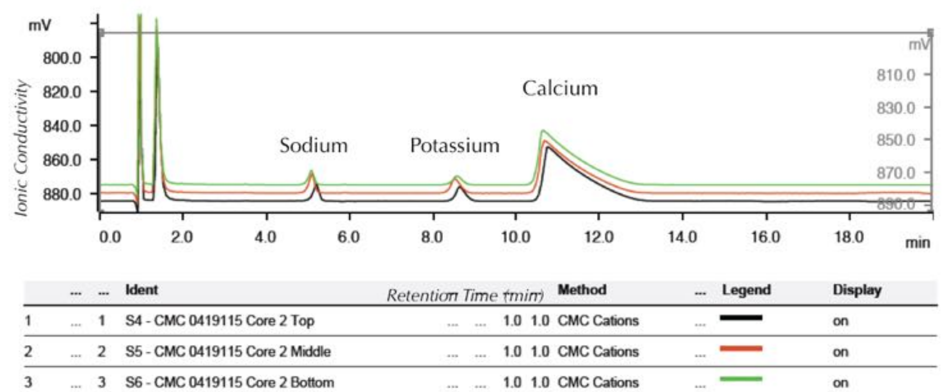

Metrohm 861 Advanced Compact IC and 788 Sample Processor, Nitric/Dipicolinic Acid eluent

Depth	Na (wt.%)	K (wt.%)	Ca (wt.%)
Top	0.018	0.043	0.398
Middle	0.018	0.043	0.382
Bottom	0.013	0.026	0.397

Cation % Weight in the Table = [(In-vial concentration from IC including Dilution Factor shown by curves, ppm) × (Original Filtrate Volume, mL)] ÷ [(Sample Weight, g) × (10,000 for ppm to wt.% conversion)]

Figure 39: Results of ion chromatography of water-soluble anions (chloride, nitrate, sulfate) at the top, and, water-soluble cations (sodium, potassium, and calcium) at the bottom of deionized water-digested pulverized concrete from the top, mid-depth, and bottom locations of Core No. 2 showing no sign of preferential enrichment of chloride, sulfate, alkalis, and calcium at the surface region compared to interior i.e. beyond the amounts detected that are judged to be from the concrete-making ingredients. Tables beneath ion chromatograms show results as percent by mass of concrete for anions and cations.

Chemical Profiles at The Top, Mid-Depth, and Bottom Locations of Core No. 3

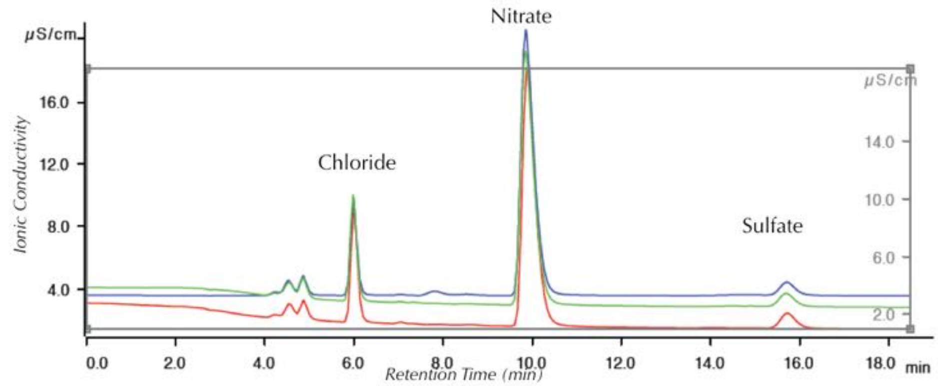

	Ident	...	Method	Analysis	Legend	Display
1	S7-CMC 0419115 Core 3 Top	... 1 ... ... 1. 1.	MVDT 4.0_Anion_UF_i-dilution by area_No D	Anions	red	on
2	S8-CMC 0419115 Core 3 Middle	... 2 ... ... 1. 1.	MVDT 4.0_Anion_UF_i-dilution by area_No D	Anions	blue	on
3	S9-CMC 0419115 Core 3 Bottom	... 3 ... ... 1. 1.	MVDT 4.0_Anion_UF_i-dilution by area_No D	Anions	green	on

Metrohm 881 Professional IC and 858 Sample Processor, in-vial dilution method, Sodium carbonate-bicarbonate eluent			
Depth	Chloride (%)	Nitrate (%)	Sulfate (%)
Top	0.006	0.065	0.001
Middle	0.004	0.067	0.001
Bottom	0.005	0.064	0.001

Anion % Weight in the Table = [(In-vial concentration from IC including Dilution Factor shown by curves, ppm) × (Original Filtrate Volume, mL)] ÷ [(Sample Weight, g) × (10,000 for ppm to wt.% conversion)]

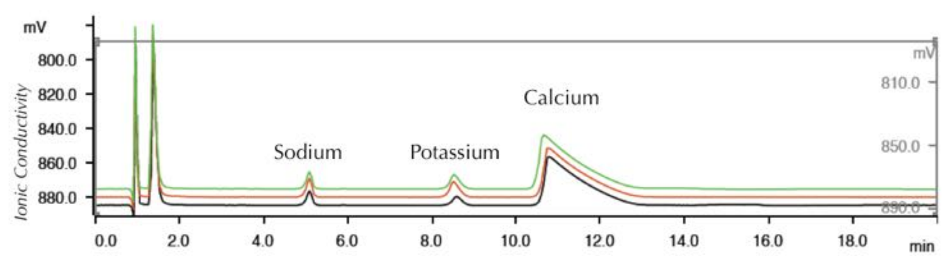

	...	...	Ident		Method	...	Legend	Display
1	...	1	S7 - CMC 0419115 Core 3 Top	... ... 1.0 1.0	CMC Cations	...	black	on
2	...	2	S8 - CMC 0419115 Core 3 Middle	... ... 1.0 1.0	CMC Cations	...	red	on
3	...	3	S9 - CMC 0419115 Core 3 Bottom	... ... 1.0 1.0	CMC Cations	...	green	on

Metrohm 861 Advanced Compact IC and 788 Sample Processor, Nitric/Dipicolinic Acid eluent			
Depth	Na (wt.%)	K (wt.%)	Ca (wt.%)
Top	0.013	0.026	0.339
Middle	0.017	0.046	0.342
Bottom	0.016	0.042	0.382

Cation % Weight in the Table = [(In-vial concentration from IC including Dilution Factor shown by curves, ppm) × (Original Filtrate Volume, mL)] ÷ [(Sample Weight, g) × (10,000 for ppm to wt.% conversion)]

Figure 40: Results of ion chromatography of water-soluble anions (chloride, nitrate, sulfate) at the top, and, water-soluble cations (sodium, potassium, and calcium) at the bottom of deionized water-digested pulverized concrete from the top, mid-depth, and bottom locations of Core No. 3 showing no sign of preferential enrichment of chloride, sulfate, alkalis, and calcium at the surface region compared to interior i.e. beyond the amounts detected that are judged to be from the concrete-making ingredients. Tables beneath ion chromatograms show results as percent by mass of concrete for anions and cations.

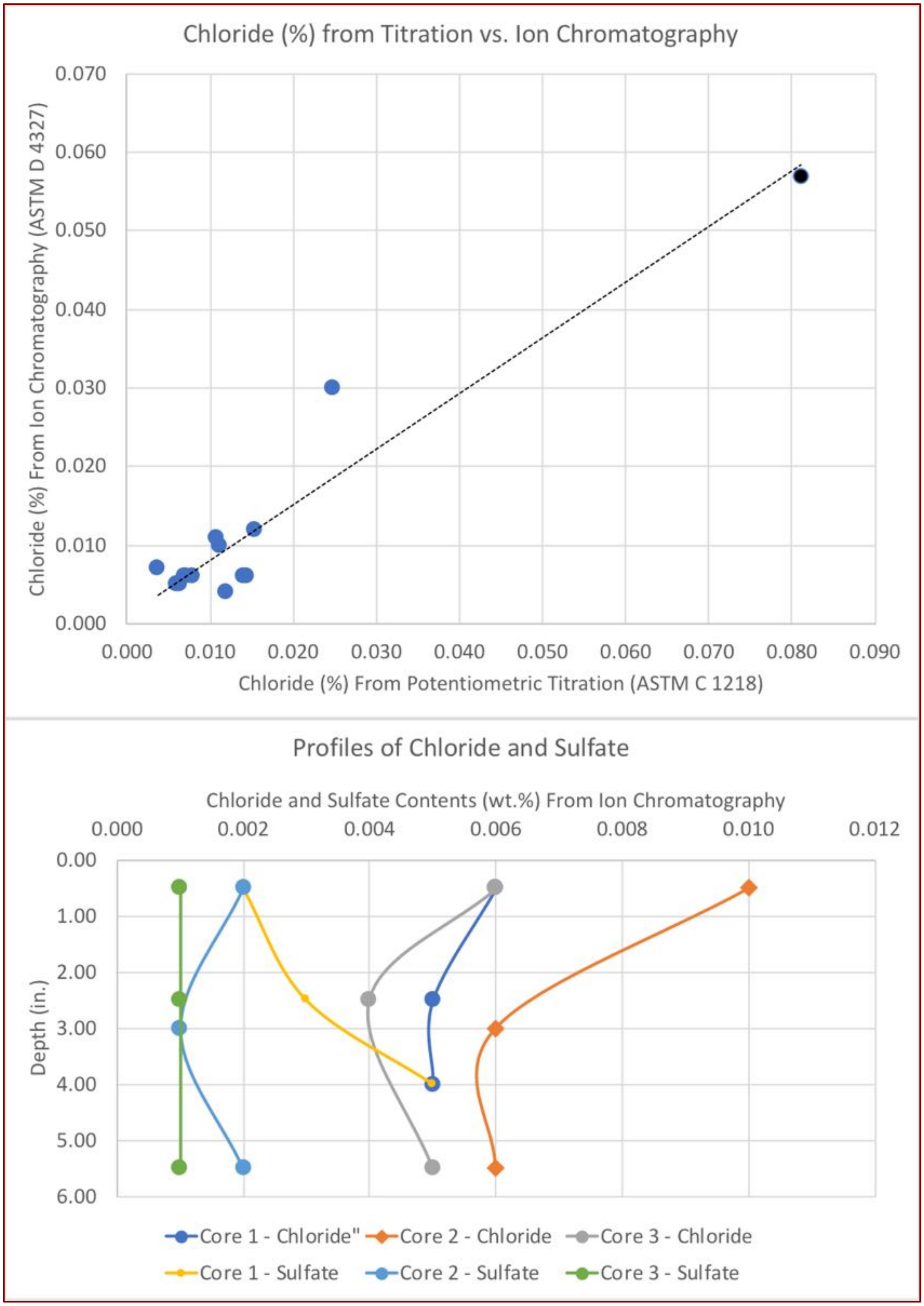

Figure 41: Top: Correlations between chloride contents from potentiometric titration (ASTM C 1218) and ion chromatography (ASTM D 4327) from the top, mid-depth, and bottom locations of the present three cores and some other data to demonstrate good correlations between two methods. Bottom: Profiles of chloride and sulfate from top, mid-depth, and bottom locations of three cores as obtained from ion chromatography.

DISCUSSIONS

DRYING SHRINKAGE, CURLING, AND CRACKING

Drying shrinkage of concrete is defined as the reduction in concrete volume from a loss of water from the concrete after hardening, and is caused principally by the contraction of the calcium silicate hydrate gel when the moisture content of the gel is decreased (Ytterberg, 1987). All practical Portland cement concrete (without reinforcement) shrinks about 400 to 800 millionths (0.0004 to 0.0008 in./in. or 0.004 to 0.008 mm/mm) due to drying in an air of 50% humidity, but when drying shrinkage is restrained by reinforcing steel, shrinkage can be reduced by up to one-half. In reinforced concrete slab with normal amounts of reinforcement, drying shrinkage is usually between 200 and 300 millionths. Similar values are found for slabs on ground restrained by subgrade. Shrinkage of cement 'paste' occurs from the loss of the 'excess' water i.e. beyond the amount needed for cement hydration, which is added to provide the workability. To fully restrain shrinkage of paste, concrete contains the maximum practical amount of incompressible, clean aggregates. Unrestrained cement paste usually shrinks about 4 to 5 times as much as concrete, which is the primary cause of shrinkage in concrete, hence is restrained by proper selection of the type, size, and grading of aggregates. The larger the maximum size of coarse aggregate, the higher is its volume in a concrete, and the lower the concrete shrinkage; hence ACI 211 recommends a large maximum-sized coarse aggregate, slightly less than $^1/_3$ the thickness of the slab to maximize the amount of aggregate and hence minimize the shrinkage.

Curling occurs when the upper part of a slab tries to occupy a smaller volume than the lower portion due to difference between the upper and lower portions with respect to shrinkage, temperature, moisture content, and other variables (Walker and Holland 1999). Upward curling slab edges and corners are caused primarily by difference in moisture content and/or temperature between the top and bottom of the slab, causing difference in drying shrinkage between the top and bottom as the top dries to a lower moisture content due to evaporation of moisture from the top than the bottom of the slab (Ytterberg, 1987; Suprenant 2002). The slab curl upwards when the surface is drier and shrinks more, or is cooler and contracts more than the bottom, e.g., when a slab is placed on a moist subgrade at the bottom, and/or exposed to low humidity air on top. For the slab to stay intact its edges must lift up, e.g., at discontinuous end of the slab, at a construction joint, a control joint, or even at a sufficiently wide crack, resulting in a loss of contact between the slab and subbase. Upward curl at slab corners can be as high as 1 in. (25 mm), but is typically about $^1/_4$ in. (6 mm). For vertically unrestrained slab corners, the panel corners must lift higher than the edges further away if no cracking is to occur. Slabs-on-grades usually curl more than the suspended slabs with the edges of the former sometimes lifted off the subgrade. Curling acts against the gravity and concrete creep, the net effect and amount of curling depends on shrinkage potential, strength, subgrade support, moisture and temperature conditions, slab thickness, joint spacing and depth, and others. Curling of edges develops substantial tensile stresses in the top of the slab (when gravity, loads, or vertical restrain tries to pull the edges down); such *curling stresses* are far more important than *linear shrinkage* in causing slab cracking. Wheeled traffic across curled edges or joints (without proper dowel load transfer) can cause spalling of cracks, joint edges, failure of joint fillers, and other problems. Unless a slab-on-grade is cast directly on a substrate that causes significant restraint (such as placement on a very uneven subgrade or an open-graded stone base), curling stresses usually far exceed linear shrinkage stresses; hence for most slab-on-grades placed on planar substrates, cracking is more due to curling stresses, or a combined effect of curling and linear shrinkage than shrinkage alone.

The term 'warping' is sometimes used to indicate upward vertical deflections from the temperature differential, and separate it from 'curling' i.e. due to moisture content (and the resultant shrinkage) differential between the top and bottom of slab. Upward deflection, however, is commonly due to the combined effects of both temperature and moisture content differentials, and thus is mostly referred to as curling.

Besides the moisture contents and resultant drying shrinkage differential between the top and bottom of slab (which is the prime factor for curling), other factors that can also contribute to curling (though not at same degree) are modulus of subgrade reaction, concrete compressive strength and modulus of elasticity, reinforcement ratio, slab thickness, joint spacing, and curing (Suprenant, 2002).

If there is no restraint during drying, shrinkage occurs freely and no stresses or cracks develop. If the tensile stress that results from restrained drying shrinkage (e.g., from aggregates, reinforcement, subgrade, etc.) exceeds the tensile strength of concrete, cracks can develop. Random cracks may develop if joints are not properly provided and the concrete is restrained from shortening. Transfer of loads or wheeled vehicular traffic across a curled free edge of a slab introduces cracking by breaking off the uplifted edge.

CONCRETE MATERIALS, MIX PROPORTIONS, & CONSTRUCTION PRACTICES

Factors that increase or decrease drying shrinkage also affect curling similarly; hence controlling the same factors can reduce both. Most early works on concrete shrinkage (Powers, 1959; Meininger, 1966; Tremper and Spellman, 1963; Ytterberg, 1987) have mentioned that water demand of the separate ingredients in concrete is the major determinant of shrinkage, hence proper choice of ingredients is the first step of combating shrinkage. Powers (1959) has mentioned six favorable materials' choices (at a given water-cement ratio) for controlling shrinkage, e.g., cement with optimum SO_3, cement with 15% retained on No. 200, less compressible aggregate (quartz), more aggregate ($1^1/_2$ in. max. size as opposed $^1/_2$ in. since latter will cause more shrinkage), and no clay in aggregate. Meininger (1966) has mentioned effects of the following factors on concrete shrinkage: source of coarse aggregate (e.g., quartz vs. greywacke, which alone could cause 100% variation in concrete shrinkage), source of fine aggregate (max. 20% effect), source of total aggregate (max. 150% effect), washing out minus No. 200 mesh, $2^1/_2$ vs. $^1/_2$ in. max. aggregate size, fine aggregate grading from coarse to fine, source of cement, cement factor, slumps, and curing. Mixture and construction practices that could increase shrinkage potential of a concrete mix include (Tremper and Spellman, 1963): (i) higher temperature of concrete at discharge, (ii) higher slump than specified, (iii) excessive haul in transit mixer, too long a waiting period at jobsite, too many revolutions at mixing speed, (iv) use of $^3/_4$ in. maximum size aggregate under conditions where 1 or 1$^1/_2$ in. size could have been used, (v) use of cement having high shrinkage characteristics, (vi) use of dirty, contaminated, or inadequately washed aggregates (due to additional fines plus increased shrinkage potential of the dirt particles), (vii) use of aggregates of poor inherent quality with respect to shrinkage, and (viii) use of an admixture that produces high shrinkage. Equivalent increase in shrinkage is 8, 10, 10, 25, 25, 25, 50, and 30 percent, respectively; the additive increase in shrinkage from all these factors can be 180 percent but the synergistic, cumulative effect can be much higher, up to 400 percent increase (Ytterberg, 1987; Walker and Holland, 1999).

The most important controllable factor affecting drying shrinkage is the amount of water per unit volume of concrete; hence shrinkage can be minimized by keeping the water content of concrete as low as possible, e.g., by keeping the coarse aggregate content as high as possible (i.e. minimizing the paste content) (Kosmatka et al., 2002). Any practice that increases the mix water content will also increase shrinkage, e.g., from making the concrete too 'soupy' (i.e. high slumps without superplastisizer), excessively high freshly mixed concrete temperatures[1], high fine-aggregate contents (or use of small-size coarse aggregate), too gap-graded, or too finely graded – the latter two reflects the importance of having as large and as evenly-graded aggregate particles as possible. The water demand of a mix at a given temperature depends on the ratio of surface area per unit volume of aggregate particles to be coated with paste (cement + water); the smaller the particle, or the more elongated and/or flat it is, the greater the ratio, and hence the greater the amount of water and cementitious materials required; therefore the greater will be the shrinkage. Some ways to reduce water content in a mix are (Tremper and Spellman, 1963): by using coarser sand, aggregates free of clay and other fine materials, avoiding finely ground high early strength cement, using cement with low C_3A content, largest possible maximum sized coarse aggregate, shortest travel time from batch plant to job site, and fewest agitating revolutions after complete mixing is achieved, and placement at lowest possible temperature (Ytterberg, 1987).

Concretes made with modern cements that are finer than older cements, many have higher C_3A contents, which may have desirable qualities for certain situations (e.g., high early strength), but many new cements shrink more than in the past. High-early strength and high-C_3A cements increase slab shrinkage (Ytterberg, 1987).

Both coarse and fine aggregates should be as well graded as possible, mostly quant or rounded in shape, have low shrinkage potential, with the fine aggregated content minimized, consistent with the required workability. Gap-grading of combined coarse and fine aggregates due to less amounts retained in many 'middle sizes' (for consumption in the asphalt industry) negatively affects shrinkage and curling potential of a slab. Use of aggregates

[1] A small amount of water can be added at the jobsite to increase workability in a hot weather construction without affecting drying shrinkage properties as long as the additions are within mix specifications (Suprenant and Malisch, 2000).

having low shrinkage potential is important to reduce concrete shrinkage since aggregates occupy the major volume (up to 70 to 75%) of normal Portland cement concrete.

Many new generations of chemical admixtures, despite providing many desirable benefits may introduce noticeable shrinkage. ASTM C 494 “Standard Specification for Chemical Admixtures in Concrete” allows up to 35 percent more shrinkage in test specimens with the admixtures than that of control specimens, which if transferred to field concrete by some mediocre admixture would require a huge reduction in water to offset this large shrinkage, or can bring undesirable admixture-related shrinkage cracking. Many high-range water-reducers added to improve workability of low *w/cm* concretes showed increased shrinkage (especially at high dosages) even though the total water content was not increased (Ytterberg, 1987). Although calcium chloride is an inexpensive set accelerator and can be used in appropriate situations, it will significantly increase shrinkage in the short and long terms (Walker and Holland 1999, Kosmatka et al., 2002). Supplementary cementing materials (e.g., fly ash) usually have little effect on shrinkage at normal dosages (Kosmatka et al., 2002).

More water in a given mix will increase shrinkage, and more cementitious materials content can have the same result (although to a lesser extent). Reducing water content by a poor quality mid or high-range water reducer at a given workability and cement content may end up in increased shrinkage than an expected reduction. Increasing compressive strength (and modulus of elasticity) either by increasing cementitious materials content (to keep *w/cm* low) and/or by reducing water content by a mediocre water-reducer can introduce undesirable shrinkage and curling.

Many early ACI and PCA literatures implied use of a low slump concrete is the key to low shrinkage. However, studies by Tremper and Spellman (1963), Meininger (1966) and Ytterberg (1987) showed that reducing slumps from 6-7 in. to 2-4 in. caused only 5-10% shrinkage reduction. Hence, slump control is only a small factor in the equation.

Significant bleeding, or upward migration of water and fines towards the top by displacing the heavier and coarser particles towards the bottom of a freshly placed concrete increases shrinkage in the top of the slab as compared to the bottom, thereby increasing curl. Minimizing water content, gap-grading, optimizing fine aggregate retained on No. 50 and 100 sieves, not placing a slab directly on a vapor retarder instead placement on an absorptive base can reduce moisture and shrinkage differential between the top and bottom from bleeding, and thus bleeding-related curling.

Placement of a slab on a moist subgrade increases slab curling, which is reduced by installing of an appropriate vapor barrier beneath the slab. A porous, permeable, dry subgrade absorbs some of the water from the base of the slab before the final set resulting in a denser lower shrinkage concrete at the slab bottom, and thus reduces curling. Cracking can occur when concrete is cast on an impervious base (e.g., polyethylene, clay, tightly compacted soil, etc.) because excess water cannot leave the slab bottom before final set.

ASTM TEST ON SHRINKAGE POTENTIAL OF A CONCRETE MIX

Due to all these above factors of concrete materials and proportions on shrinkage for a given mix, it is best to test the shrinkage potential of a mix by ASTM C 157 (or AASHTO T 160).

COMPRESSIVE STRENGTH AND MODULUS OF ELASTICITY

High strength concretes generally (but not always) shrink more and always have a higher modulus of elasticity. The modulus of elasticity is a very important factor because the higher the modulus the more curl will occur and the less the curled edged will relax downward over time due to creep (Walker and Holland, 1999). Many studies have clearly shown that curling is directly proportional to modulus of elasticity (Suprenant, 2002). It is reasonable to estimate from a designer's perspective that increasing the required concrete strength by 1000 psi (6.9 MPa) i.e. increasing the modulus of elasticity by about 10% increases curling deflections by about 10%. Compressive strength should be no greater than designed, or any 'excess' strength can be detrimental with respect to shrinkage and curling. Higher than necessary 28-day minimum strength requirements for many industrial floor slab on grade magnifies shrinkage problems (Ytterberg, 1987). For an industrial floor anticipating heavy traffic and high abrasion, a moderate strength (3000-4000 psi) concrete with a mineral or metallic aggregate surface hardener can actually provide better surface durability and less potential to shrinkage, curling, and cracking than a slab designed with a higher strength concrete for the anticipated traffic (Holland and Walker 1998).

For the present slab, the reported design strength of 3500-psi is exceeded by as much as 170 percent in the 28-day cylinder strengths of concrete (e.g., around 6000 psi) which has not only increased the modulus of elasticity of concrete but also the curling and curling-related differential drying shrinkage potential of the slab and hence cracking from curling and differential shrinkage.

REINFORCING STEEL

Cracks in a slab-on-grade floor surface are wider at the top than at bottom. For the best crack control and limit crack width, therefore, reinforcing steel should be as close to the slab surface as possible (without causing plastic settlement cracks over the steel), preferably within the top half to top one-third the total thickness of a slab. Since it is the upper half of a slab on grade that has the greatest shrinkage, the reinforcement should be as close as possible to the top of the slab (but not closer than $1^1/_2$ in.) in order to restrain the shrinkage and reduce curling (Ytterberg, 1987). By contrast, reinforcement in the bottom half of slabs on grade will actually increase curling because it further restrains the already low shrinkage of the bottom half of the slab. For a 5-in. thick slab, it is preferred to use #4 bars near the top with 1-inch thick cover, or #5 bars with 1.5 inch cover (Holland and Walker 1998). For #5 bars, greater cover depth is needed to control plastic settlement cracking over the bar. ACI Committee 302 recommends using 1% reinforcement that extends perpendicularly about 10 ft. (3 m) from the slab edge or construction joint towards the center; 1% reinforcement could decrease curling deflection by about 60 to 80% (Suprenant, 2002).

SLAB THICKNESS

Curling is greatest at corners of slabs, and corner curling is reduced as slab thickness increases. For example, a 2-in. increase in slab thickness can reduce corner curling by more than 50% (Suprenant, 2002).

JOINT SPACING AND DEPTH

Minimizing joint spacing can greatly decrease curl and the resultant cracking. For unreinforced or lightly reinforced slabs, the commonly used joint spacing criteria of 24 to 36 times the slab thickness (or 2 to 3 times the thickness of the slab but in feet) can be unconservative for many of today's concretes, especially as slab thickness increases. It is true that the thicker the slab, the longer the joint spacing can be; however, it is not a linear relationship. For unreinforced or lightly reinforced slabs, joint spacing should not exceed 15 ft. (4.6 m) for a 5-in. thick slab. For control joints to be effective as plane of weakness (i.e. for the cracks to be controlled and form beneath those joints than elsewhere), joints should be cut or tooled to depths of one-forth (25 percent) the thickness of the slab, and distributed steel reinforcement must be discontinued at control joints (PCA, 1983). There will be a marked loss of effectiveness of aggregate interlock at shrinkage control joints in the slab if the joints are spaced more than 15 ft. apart; for effective crack control joint spacing should be 12 to 18 ft. for a 6-in. thick slab on grade (PCA).

The present slab is reported to have joint spacings of 12 to 13 ft. and saw-cut depths of 1.5 to 2 inches. For a slab thickness of 5 to 6 inches, these reported joint spacings and depths are acceptable.

OTHER FACTORS

Other ways to minimize curling and cracking are to use properly designed and constructed slabs with continuous reinforcement (mild steel or steel fibers) and no contraction joints, shrinkage-compensating concrete, or post-tensioning.

Both concrete and ambient temperatures at placement should be as low as feasible to minimize shrinkage, surface drying, and thermal contraction from cooling. Proper curing is also important especially in the first few hours after placement to prevent excessive drying between and immediately after finishing.

Curing prevents drying out of surface and promotes adequate cement hydration at the surface by providing optimum temperature and moisture for cement hydration without which dusting or fine, hair-like shallow-depth craze cracking of the surface commonly occurs. Curing, however, does not reduce total shrinkage or shrinkage differential between the top and bottom of slab; thus duration of curing has no effect on whether a slab with curl or how much it will curl, but the duration of curing may influence when a slab will curl, extended curing only delays drying shrinkage and curling, it does not reduce shrinkage or curling (ACI Committee 360, Suprenant, 2002, Kosmatka et al. 2002). Shrinkage from carbonation of surface only affects the top few millimeters of a well-consolidated slab, which is insufficient to cause curling, or major shrinkage-related cracking (Ytterberg, 1987).

After proper curing, moisture content differential between the top and the bottom of the slab can be minimized by using coatings, sealers, etc., which will also minimize carbonation, which adds to surface shrinkage. Minimizing curling is important for slabs anticipating heavy loads, vehicular traffic (to prevent cracking of curled edges lacking support from the subgrade), or for slabs receiving topping or floor covering.

Air conditioning and increased heating requirements in many indoor buildings tend to lower relative humidity of ambient air and thus increase slab curl and shrinkage. Placement of slabs on a moist subgrade without a vapor barrier, or with a mediocre vapor retarder, or one that has been poorly installed and/or damaged during construction can introduce differential moisture conditions between the slab top and bottom surfaces and thus introduce curling.

The rate and ultimate amount of shrinkage are usually smaller for larger masses of concrete than for small masses; on the other hand, shrinkage continues longer for large masses. Higher volume-to-surface ratios (larger elements) experience lower shrinkage (Kosmatka et al., 2002).

CONCLUSIONS

Based on: (i) review of field photographs and background information provided with the sample; (ii) examination of field photographs of concrete surface cracking, (iii) examination of the configuration of the major visible vertical through-depth crack in Cores 1 and 3, (iv) petrographic examination of sound condition of the concrete away from the crack with no evidence of any chemical deteriorations to cause the crack in the first place, (v) along with sound condition of concrete ingredients and normal mix proportions (cement content water-cement ratio, etc.), where neither the concrete materials nor the proportions have contributed to the cracking, *the observed and reported cracking in the concrete slab was judged to be due to accommodative drying shrinkage of concrete, which may or may not have been aggravated by some additional curling of the slab due to differential drying shrinkage between the top and bottom surfaces of the slab, along with possible early freezing of a non-air-entrained concrete after placement in a winter weather condition without any reported heated enclosures*.

Reasons that could contribute to drying shrinkage and/or curling-related cracking, and, early freezing-related cracking of the slab include:

a. Differential shrinkage of the concrete at the top and bottom ends and possible curling of the slab, especially if the slab was exposed to temperature and/or moisture differential between the top and bottom surfaces, i.e. if the slab was exposed to open air for moisture evaporation (especially in a hot, windy, or dry environment), and was not protected or prevented from moisture loss at the top finished surface region, especially when the slab was placed on a vapor retarder to prevent any moisture loss at the bottom end except only through the top thus to create a moisture gradient, where there is no possibility of drying of the slab from the bottom end as fast as from the top; hence, differential drying was quite possible under the situation, which could have led to the observed cracking of the slab;

b. Inadequate presence, wide spacing, shallow depths, or late placement of control joints in the slab, which were either inactive or did not effectively control shrinkage-related cracking at the joint locations rather than elsewhere in the slab, which has caused development of visible major shrinkage cracks in the slab. For an observed 5 to 6 in. thickness of the slab (from the thicknesses of the cores), the reported 12 to 13 ft. spacing of control joint and 1.5 to 2 in. depths of joints are acceptable. However, deviations from the reported spacing and/or depths of joint could contribute to some uncontrolled shrinkage cracking.
c. Inadequate amount of wire mesh and steel reinforcement in the slab, especially due to the absence of any mesh or reinforcing steel in the cores examined. Presence of polypropylene-type fiber reinforcement in the concrete however should provide some resistance to shrinkage-related cracking.
d. The reported compressive strength test results of cylinders are around 6000 psi at 28 days, i.e. noticeably higher than the reported 28-day design strength of 3500 psi. Such higher than needed strength would increase the modulus of elasticity of concrete, which would increase the potential for curling and curling-related cracking of slab.
e. The reported mix design of the concrete called for a non-air-entrained concrete, which if supplied to areas not well protected from freezing during November 2018 placement could have developed some freezing-relate cracking especially the near-surface cracks found within the top 1 in. in Cores 2 and 3.
f. Any other non-concrete-related reasons, which are not possible to investigate from the present study.

From the present study, the concrete materials *per se* are judged to be sound and did not contribute to the cracking.

REFERENCES

ACI Committee 211, "Standard Practice For Selecting Proportions for Normal, Heavyweight, and Mass Concrete," American Concrete Institute, Farmington Hills, Michigan, 2014.

ACI Committee 224, "Control of Cracking in Concrete Structures." American Concrete Institute, Farmington Hills, Michigan, 2014.

ACI Committee 302, "Guide for Concrete Floor and Slab Construction," American Concrete Institute, Farmington Hills, Michigan, 2014.

ACI Committee 360, "Design of Slabs on Grade," American Concrete Institute, Farmington Hills, Michigan, 2014.

ASTM C 856 "Standard Practice for Petrographic Examination of Hardened Concrete," Vol. 4.02, ASTM International, West Conshohocken, PA, 2014.

Holland, J.A., and Walker, W., "Controlling Curling and Cracking in Floors to receive coverings," Concrete Construction, July 1998,

Jana, D., and Cole, A.A., Microscopy: A Practical Solution to Concrete Problems, Bulletin of Concrete Industry Board, September 1997, pp. 18-22.

Jana, D., Petrography: A Powerful Tool For Solving Common Concrete Problems, Civil Engineering NEWS, March 1997, pp. 40-44.

Jana, D., Sample Preparation Techniques in Petrographic Examinations of Construction Materials: A State-of-the-art Review, Proceedings of the 28th Conference on Cement Microscopy, International Cement Microcopy Association, Denver, Colorado, pp. 23-70, 2006.

Jana, D., Concrete, Construction, or Salt – Which Causes Scaling? Part 2: Importance of Finishing Practices; Concrete International, December 2004, pp. 51-56, American Concrete Institute.

Jana, D., Petrography and Concrete Repair – A Link is Needed, Point of View Publication in Concrete International, American Concrete Institute, pp. 37-39, January 2005.

Jana, D., and Erlin, B, Delamination – The Sometime Curse of Entrained Air, Concrete Construction, January 2005, pp. 101-106.

Kosmatka, S.H., Kerkhoff, B., and Panarese, W.C., Design and Control of Concrete Mixtures, 14th Edition, Engineering Bulletin 001, Portland Cement Association, 2002.

Meininger, R.C., "Drying Shrinkage of Concrete," Engineering Report No. RD3, National Ready Mixed Concrete Association, 22pp., 1966.

Portland Cement Association, "Concrete Floors on Ground," 2nd Edition, Publication No. PA136B, 16 pp, 1983.

Powers, T.C., "Causes and Control of Volume Change," Journal, PCA Research and Development Laboratories, V. 1, No. 1, pp. 29-39, 1959.

Peterson, K.R., Swartz, R.A., Sutter, L.L., and Van Dam, T.J., "Air Void Analyses of Hardened Concrete with a High-Resolution Flatbed Scanner," Proceedings of 24th International Conference on Cement Microcopy, San Diego, CA, pp. 304-316, 2002.

Peterson K., Sutter L., Radlinski M. "The practical of application a flatbed scanner for air-void characterization of hardened concrete" Journal of ASTM International, v 6, n 9, October 2009.

Peterson K., Anzalone G., Nezami S., Oh C., Lu H., "Robust Test of the Flatbed Scanner for Air-Void Characterization in Hardened Concrete" ASTM Journal of Testing and Engineering, v 44, n 1, January 2016.

Suprenant, B.A., "Why slabs curl, Part I," Concrete International, March 2002.

Suprenant, B.A., "Why slabs curl, Part II," Concrete International, April 2002.

Suprenant, B.A., and Malisch, W.R., "A new look at water, slumps, and shrinkage," Concrete Construction, Addison, Illinois, pp. 48-53, 2000.

Tremper, B., and Spellman, D.L., "Shrinkage of Concrete – Comparisons of Laboratory and Field Performance," Highway Research Record No. 3, Highway Research Board, pp. 30-61, 1963.

Walker, W.W., and Holland, J.A., "Thou shalt not curl nor crack….(hopefully)," Concrete Construction, Jan. 1999

Ytterberg, R.F., "Shrinkage and curling of slabs on grade, Part 1," Concrete International, April 1987.

Ytterberg, R.F., "Shrinkage and curling of slabs on grade, Part 2," Concrete International, May 1987.

Ytterberg, R.F., "Shrinkage and curling of slabs on grade, Part 3," Concrete International, June 1987.

✪ ✪ ✪ END OF TEXT ✪ ✪ ✪

END OF REPORT[2]

[2] The CMC logo is made using a lapped polished section of a 1930's concrete from an underground tunnel in the U.S. Capitol.